(U) SUMMARY OF THE ALTITUDE DEVELOPMENT TESTING OF THE BELL MODEL 8258 ROCKET ENGINE IN THE PROPULSION ENGINE TEST CELL (J-2A) (LEM ASCENT STAGE PRIMARY PROPULSION SYSTEM)

E. H. Matkins and K. L. Farrow
ARO, Inc.

June 1965

ROCKET TEST FACILITY
ARNOLD ENGINEERING DEVELOPMENT CENTER
AIR FORCE SYSTEMS COMMAND
ARNOLD AIR FORCE STATION, TENNESSEE

NOTICES

When U. S. Government drawings specifications, or other data are used for any purpose other than a definitely related Government procurement operation, the Government thereby incurs no responsibility nor any obligation whatsoever, and the fact that the Government may have formulated, furnished, or in any way supplied the said drawings, specifications, or other data, is not to be regarded by implication or otherwise, or in any manner licensing the holder or any other person or corporation, or conveying any rights or permission to manufacture, use, or sell any patented invention that may in any way be related thereto.

Qualified users may obtain copies of this report from the Defense Documentation Center.

This document contains information affecting the national defense of the United States within the meaning of the Espionage Laws (Title 18, U.S.C., Sections 793 and 794) the transmission or revelation of which in any manner to an unauthorized person is prohibited by law.

References to named commercial products in this report are not to be considered in any sense as an endorsement of the product by the United States Air Force or the Government.

Do not return this copy. When not needed, destroy in accordance with pertinent security regulations.

AEDC-TR-65-97

(U) SUMMARY OF THE ALTITUDE DEVELOPMENT TESTING OF THE BELL MODEL 8258 ROCKET ENGINE IN THE PROPULSION ENGINE TEST CELL (J-2A) (LEM ASCENT STAGE PRIMARY PROPULSION SYSTEM)

E. H. Matkins and K. L. Farrow
ARO, Inc.

FOREWORD

(U) The work reported herein was done at the request of the Manned Spacecraft Center (MSC), National Aeronautics and Space Administration (NASA) for the Bell Aerosystems Company (BAC) under Program Area 921E, Project 9071.

(U) The results of the tests were obtained by ARO, Inc. (a subsidiary of Sverdrup and Parcel, Inc.), contract operator of the Arnold Engineering Development Center (AEDC), Air Force Systems Command (AFSC), Arnold Air Force Station, Tennessee, under Contract AF40(600)-1000. The test was conducted from May 28 to September 15, 1964, in the Propulsion Engine Test Cell (J-2A) of the Rocket Test Facility under ARO Project Number RL1422, and the report was submitted by the authors on April 27, 1965.

(U) This report contains classified information extracted from the following reports:

1. AEDC-TDR-64-211, October 1964 (Confidential, Group 4)
2. AEDC-TDR-64-242, November 1964 (Confidential, Group 4)
3. AEDC-TDR-64-258, November 1964 (Confidential, Group 4)
4. BAC Report Number 8258-927003, March 1964 (Confidential, Group 4)

(U) This technical report has been reviewed and is approved.

Ralph W. Everett
Major, USAF
AF Representative, RTF
DCS/Test

Jean A. Jack
Colonel, USAF
DCS/Test

[redacted]ABSTRACT

(C) The development test program of the LEM Ascent Stage Primary Propulsion System was conducted in the Propulsion Engine Test Cell (J-2A). This program was designed to determine the performance, thermal characteristics, and durability of two configurations of the engine at a pressure altitude of approximately 100,000 ft. One configuration of the engine was operated at a chamber pressure of 100 psia and the other at 120 psia. Included in the program were (1) a simulated mission duty cycle for both configurations of the all-ablative engines, (2) a survey of engine performance as a function of chamber pressure, chamber length, and mixture ratio utilizing an all-metal engine of the 120-psia chamber pressure configuration, and (3) a study of the proposed LEM Ascent Staging technique using an all-ablative 120-psia chamber pressure engine. The results of the program indicated that the mean value of vacuum specific impulse, characteristic velocity, vacuum thrust coefficient, and the mass ablation for the 120-psia chamber pressure configuration were 309.5 lb_f-sec/lb_m, 5471 ft/sec, 1.820, and 0.0336 lb_m/sec, respectively. The vacuum specific impulse obtained at 120-psia chamber pressure was approximately 1 percent higher than that obtained at 100 psia. The performance of the two configurations was comparable when corrected to the same area ratio, chamber pressure, mixture ratio, and chamber length. The structural integrity of the engine was demonstrated by the successful completion of the mission duty cycle and the simulated vehicle staging tests.

CONTENTS

ILLUSTRATIONS

TABLES

SECTION I
INTRODUCTION

(U) The Apollo vehicle consists of a Command Module (C/M) (three-man capsule), a Service Module (S/M), and a Lunar Excursion Module (LEM). The mission of the LEM is to ferry astronauts to and from the lunar surface. The LEM consists of two stages: a Descent Stage to provide a soft landing on the lunar surface and an Ascent Stage for takeoff from the lunar surface and rendezvous with the Apollo Command Module in lunar orbit.

(U) An engine development program of the LEM Ascent Stage Primary Propulsion system was conducted in the Propulsion Engine Test Cell (J-2A) of the Rocket Test Facility. The test program was divided into four phases with the following primary objectives:

Phase I - Determination of engine performance and ablation characteristics of two different types of all-ablative, thrust-chamber-nozzle assemblies. The results of this phase of testing are reported in Ref. 1.

Phase II - Determination of the effect on engine performance of chamber pressure variations of 100, 120, and 140 psia over a mixture ratio range of from 1.4 to 2.1 using an all-metal, water-cooled, thrust-chamber-nozzle assembly with characteristic lengths of 30 and 42 in. The results of this phase of testing are reported in Ref. 2.

Phase III - Determination of engine performance during a simulated mission duty cycle utilizing the final configuration of the LEM Ascent engine thrust-chamber-nozzle assembly. The results of this phase of testing are reported in Ref. 3.

Phase IV - Evaluation of the proposed LEM Ascent vehicle staging technique. The results of this phase of testing are presented in Ref. 4.

(U) This report presents a summary of the results of these four phases of testing as reported in Refs. 1 through 4 and also presents a comparison of the performance of the 100-psia chamber pressure engine tested during Phase I with that of the 120-psia chamber pressure engine tested during Phase III. This performance comparison is based on the results of the Phase II tests which included variations in chamber pressure,

mixture ratio, and chamber length. Included in these comparisons are adjustments for differences in heat loss and expansion ratio.

SECTION II
APPARATUS

2.1 TEST ARTICLES

(C) The BAC Model 8258 rocket engine (Fig. 1) is a pressure-fed, bipropellant engine which uses the hypergolic propellants nitrogen tetroxide (N_2O_4) as the oxidizer and equal gravimetric parts of hydrazine (N_2H_2) and unsymmetrical dimethylhydrazine $[(N_2H_2)(CH_3)_2]$ as the fuel at a nominal mixture ratio of 1.6. The engine is designed for multiple firings in a space environment for a total of 455 sec (maximum of 35 firings). The maximum duration for any single firing is 380 sec (Ref. 5).

(C) The engine consists of an injector, ablative-thrust-chamber-nozzle assembly, bipropellant valve, and electrical control harness. The bipropellant valve and electrical control harness were not used during the first three phases of this program; instead, facility propellant valves and electrical control wiring were used. The fourth phase of this program incorporated a prototype bipropellant valve (Ref. 4) but not the electrical control harness. All engines used in this program were designed to develop a nominal 3500-lb thrust. The engines utilized in Phase I were designed to develop a nominal vacuum specific impulse of 306.3 lb_f-sec/lb_m at a chamber pressure of 100 psia, whereas the engines utilized during the remainder of the program were designed to develop 308.3 lb_f-sec/lb_m at 120 psia.

(U) Table I lists the various engine components that were used during this program.

2.1.1 Thrust-Chamber-Nozzle Assemblies

(C) The BAC Model 8258 rocket engine utilized during the Phase I testing of this program incorporated an all-ablative, thrust-chamber-nozzle assembly with an area ratio of 40:1 and was designed to operate at 100-psia chamber pressure. One assembly, fabricated by the AVCO Corporation (AVCO) was used during Test No. 01 (Fig. 2a). Three assemblies, manufactured by the H. I. Thompson Company (HITCO), were used during Tests No. 02, 03, and 04 (Figs. 2b and c). The HITCO assembly used during Test No. 02 differed from the assemblies used during Tests 03 and 04 in that the insulation layer ended at the 6:1 area

ratio just downstream of the nozzle throat. The materials used in the manufacture of the Phase I chambers are given in detail in Ref. 1.

(C) Phase II tests were conducted using an all-aluminum, water-cooled, thrust chamber and nozzle throat section. A radiation-cooled stainless steel nozzle extension was attached at the 7:1 area ratio and extended to an area ratio of 45.6:1 (Fig. 2d). This chamber was dimensionally identical to the all-ablative, thrust-chamber-nozzle assembly tested in Phase III. Detailed information on the Phase II assembly is contained in Ref. 2.

(C) Three all-ablative, thrust-chamber-nozzle assemblies with area ratios of 45.6:1 and designed to operate at 120-psia chamber pressure were tested during Phase III (Fig. 2e). These assemblies were dimensionally similar to the Phase I assemblies except that the throat area was smaller. These chambers were also different from those used in Phase I in that the material which was used to insulate the chamber and throat section was also used as the ablative layer from the 6:1 area ratio to the 45.6:1 area ratio. Further construction details are presented in Ref. 3.

(U) The Phase IV tests were conducted utilizing one thrust-chamber-nozzle assembly identical to the assemblies used during Phase III.

(U) The first three tests of Phase I (Tests No. 01, 02, and 03) and the last series of tests of Phase II (Test B3) were conducted utilizing a 4.125-in.-long, water-cooled combustion chamber extension (Fig. 3). This assembly was used during Phase I to prevent excessive grooving of the thrust chamber wall near the injector. This section was also used during Phase II to effect a change in the chamber characteristic length.

2.1.2 Injectors

(C) Two types of injectors, Series A and B (Fig. 4), were utilized during this test program. Tests No. 01, 02, and 03 of Phase I used a Series A injector. This injector had 40 doublet orifices on the periphery to provide film cooling of the chamber wall and 140 triplet primary orifices arranged in a square pattern. The remainder of the test program (Test No. 04 of Phase I, Phase II, Phase III, and Phase IV) utilized the Series B injector. This injector contained 96 doublet orifices on the periphery for film cooling and 92 triplet primary orifices arranged in concentric circle patterns.

(U) Two types of Series B injectors were used in Phase II testing. The only difference was in the orifice hole size. This difference had no effect on engine performance as indicated in Ref. 2.

2.2 INSTALLATION

(U) The test program was conducted in the Propulsion Engine Test Cell (J-2A) (Fig. 5), which is a propulsion chamber designed to simulate pressure altitudes in excess of 350,000 ft. The test cell consists of an 18-ft-diam, 30-ft-long stainless steel thermopanel liner installed within the 20-ft-diam basic test cell ducting and is equipped with mechanical and cryogenic pumping systems and an exhaust gas ejector-diffuser. However, the only pumping systems used for the tests reported herein were the mechanical vacuum pumps and the exhaust gas ejector-diffuser in series with the facility exhausters.

(U) The engines were mounted on the thrust cradle, which is supported from the cradle support stand by two vertical and three horizontal double universal flexure assemblies (Fig. 5a). Axial movement of the thrust cradle was restrained by a thrust butt through a load cell train.

(U) A 15-ft-long cylindrical supersonic diffuser with an inlet diameter of 45 in. and a 36-in.-diam second throat was used to compress the engine exhaust gases and to maintain altitude conditions during rocket firings. The inlet plane of the supersonic diffuser was positioned 2.75 in. downstream of the engine nozzle exit plane. The exhaust gases from the diffuser were discharged into facility exhaust ducting and were removed by the RTF exhauster system (Ref. 6).

(U) Two valves are used to provide the test cell with an engine restart capability: a hydraulically operated, 6-ft-diam restart valve and a hydraulically actuated diffuser valve (Fig. 5). A disc is used in the restart valve to seal the test cell (which is normally at a lower pressure) from the RTF exhaust duct pressure when the diffuser valve is open. The 6-ft-diam restart valve was located downstream of the diffuser and consisted of two 20-mil Mylar® discs mounted in steel rings, a hydraulic actuation system, and a pyrotechnic system. One 6-ft-diam disc was positioned in the duct downstream of the diffuser, while the other disc remained inside the 20-ft-diam basic test cell exhaust duct. At the beginning of a rocket firing, the disc in the 6-ft-diam duct was severed by the pyrotechnic system and was discharged from the duct by the rocket exhaust. After the firing, the restart valve was remotely operated to insert the remaining disc from the cell exhaust duct into the 6-ft-diam exhaust duct. The diffuser valve was installed to prevent atmospheric air pressure from rupturing the Mylar disc in the 6-ft-diam duct during periods when the RTF exhauster system was not in operation.

(U) During Phase IV testing, a 60-in.-diam steel plate was installed downstream of the nozzle exit (Fig. 5b). The axial location of the plate

relative to the nozzle exit was adjusted manually between test periods, and the angular position was controlled remotely from the control room between the test firings. The exhaust gases from the engine were discharged into the test cell, flowed around the plate at the nozzle exit, through the exhaust gas diffuser, and were removed by the RTF exhaust system (Ref. 6).

(U) Each propellant system for the engine consisted of an insulated 1000-gal stainless steel tank, a tank filling system, a nitrogen pressurizing and regulating system, filters, and associated valving (Fig. 6). For the first three phases of testing, two 2-in.-diam, air-operated valves were installed approximately 24 in. upstream of the injector and were used as engine propellant valves. Two turbine-type flowmeters were installed in series in each propellant line outside the test cell for flow measurement. The fourth phase of testing utilized a fast acting bipropellant valve (supplied by BAC) similar in operation to the proposed flight valve. This valve permitted firings of less than one second as required for this phase of testing.

2.3 INSTRUMENTATION

(U) Instrumentation was provided to obtain measurements of axial thrust, engine and test cell pressures, propellant pressures and flow rates, and engine and propellant temperatures. Visual coverage of the engine during operation was provided by closed-circuit television and motion-picture cameras.

2.3.1 Pressure

(U) Thrust chamber pressures were measured with strain-gage-type transducers located approximately one foot from the engine. The number of chamber pressure transducers utilized were: Phase I, three; Phase II, six; Phase III, four; and Phase IV, one. The transducers were manifolded, and the manifold was connected to the pressure tap. The chamber pressure measurements were taken at a tap located in the center of the injector except for Phase II. For this phase, three were taken at the injector and three at a tap in the chamber wall located immediately upstream of the converging section of the nozzle (Ref. 2).

(U) Strain-gage-type transducers were also used in each propellant system to measure tank pressures, feed pressures, injector inlet pressures, and differential pressures across the injector (Fig. 6). In addition to the above measurements which were taken on all four phases of testing, Phase II and IV test articles were fitted with strain-gage-type transducers connected to nozzle static pressure taps.

(U) The outputs of the strain-gage-type transducers were recorded in frequency form on magnetic tape and in analog form on light-beam oscillographs and null-balance potentiometers.

(U) Test cell pressures were measured with variable capacitance-type transducers (Fig. 5) and were recorded in frequency form on magnetic tape and in analog form on a null-balance potentiometer.

(U) All transducers were laboratory calibrated with a secondary standard before and after each phase of testing. Before, during, and at the end of each test period, the pressure transducers were calibrated by an electrical four-step calibration using resistances in the transducer circuits to simulate selected pressure levels.

2.3.2 Temperatures

(U) Temperatures were measured on the engine with Chromel® - Alumel® thermocouples. The exact locations and number of thermocouples are presented in Refs. 1 through 4. The electrical outputs from these thermocouples were recorded on null-balance potentiometers or in digital form on magnetic tape by an analog-to-digital commutating data system. The data recorded were converted to degrees and tabulated by a digital computer.

(U) Immersion-type thermocouples were used in each propellant system to measure propellant temperatures in the tank, near the propellant valve, and at the injector inlet. Propellant temperatures at the flowmeters were measured by resistance temperature transducers, recorded in frequency form on magnetic tape, converted to degrees, and tabulated by a digital computer.

2.3.3 Flow Rates

(U) Two turbine-type flowmeters were installed in each of the propellant feed lines to measure propellant flow rates. The flow rates were recorded in frequency form on magnetic tape and light-beam oscillograph and in analog form on null-balance potentiometers. Prior to the testing of each phase of the program, the flowmeters were bench calibrated using water. At least one flowmeter in each propellant system was calibrated using the particular propellant as the flowing fluid. The flow measurement recording systems were calibrated before, during, and after each test period by applying a known frequency which simulates a selected flowmeter output.

(U) Two turbine-type flowmeters were installed in each of the cooling-water discharge lines to measure cooling water flow rates on the Phase II configuration engine (Fig. 2d).

2.3.4 Miscellaneous

(U) In addition to the above mentioned instrumentation, engine instrumentation for Phase IV also included nozzle vibration and engine strain sensors at several specific locations (Ref. 4).

2.3.5 Instrumentation Accuracy

(U) The accuracy of the measured steady-state engine data obtained during the first three phases of the LEM Ascent test in the Propulsion Engine Test Cell (J-2A) has been determined (Ref. 7) and is stated for three standard deviations (3σ) as a percentage of the steady-state value.

Parameter	3σ
Thrust, F	0.303
Chamber Pressure, P_c (Lab Calibrations)	0.594
Chamber Pressure, P_c (In-Place Calibrations)	0.549
Propellant Flow Rate, W_T	0.375
Throat Area, A_T	0.006
Nozzle Exit Area, A_{ne}	0.012

(U) The errors of the calculated engine performance parameters, F_∞, C_F, C_{F_∞}, I_{sp_∞}, and c* from the measured data were:

Parameter	P_c(In-Place Calibrations) 3σ	P_c(Lab Calibrations) 3σ
Vacuum Thrust, F_∞	0.330	0.330
Thrust Coefficient, C_F	0.627	0.666
Vacuum Thrust Coefficient, C_{F_∞}	0.642	0.678
Vacuum Specific Impulse, I_{sp_∞}	0.498	0.498
Characteristic Velocity, c*	0.666	0.702

The above errors are the combined statistical sum of the random and systematic errors.

(U) The accuracy of the Chromel-Alumel thermocouple data, including the analog-to-digital computing system, is estimated to be ±3.0 percent. The accuracy of the temperature measurements recorded on magnetic tape in frequency form and on continuous recording null-balance potentiometers is estimated to be ±1.0 percent.

SECTION III
PROCEDURE

3.1 TESTING

(U) The test program was divided into four separate phases. The firing sequence for each phase is included in Table I. The detailed procedures for each phase of testing can be found in Refs. 1 through 4.

3.2 DATA REDUCTION

(U) Measurements of engine thrust, chamber pressures, test cell pressure, propellant pressures, propellant temperatures, and flow rates were recorded on magnetic tape as a frequency and were translated into digital form for Phases I, II, and III. An average value of each parameter was computed by an IBM 7074 computer at 1.0-sec intervals for each test except for the short-duration firings of Phase I, which were averaged over a 0.2-sec interval. All other temperature measurements were recorded in digital form on magnetic tape and were converted to degrees and tabulated at 1.0-sec intervals by a digital computer. The computer also provided a graph of the variation of each temperature as a function of time.

(U) During the Phase IV testing, measurements of engine thrust, combustion chamber pressure, nozzle static pressure, and engine strain were recorded on magnetic tape in frequency form and were transcribed into digital form. One average value of each parameter was computed and tabulated by an IBM 7074 electronic computer at 0.005- and 0.025-sec intervals for each firing.

(U) Engine performance data were calculated from the higher accuracy data obtained from the frequency-modulated magnetic tape system for Phases I, II, and III. An IBM 7074 computer was programmed to use the measured data samples to compute engine performance parameters at 1-sec intervals throughout the 380-sec firings of Phase I, all the firings of Phase II, and the 60- and 30-sec firings of Phase III. No performance data were calculated for the Phase IV firings.

(U) Vacuum thrust (F_∞), specific impulse (I_{sp_∞}), and thrust coefficient (C_{F_∞}) were calculated by the computer from the measured data.

(U) Characteristic velocity (c*) for the thrust chamber was calculated as follows:

$$c^*_j = \frac{P_{c_j} A_{T_i} g}{\dot{W}_T} \tag{1}$$

or

$$c^*_n = \frac{P_{c_n} A_{T_i} g}{\dot{W}_T} \tag{2}$$

where

P_{c_j} is the thrust chamber pressure measured at the injector,

P_{c_n} is the thrust chamber pressure measured at the nozzle entrance,

A_{T_i} is the measured pre-fire throat area,

g is the dimensional constant (32.174 $lb_m ft/lb_f sec^2$),

$\dot{W}_T$ is the total propellant flow rate.

The corrected characteristic velocity was calculated as follows:

$$c^*_{corr} = \frac{P_{cc} A_{T_i} g}{\dot{W}_T} \tag{3}$$

where

P_{cc} is the thrust chamber static pressure measurement corrected to the throat total pressure.

The corrections supplied by BAC were 0.98621 x P_{c_j} (used for Phase I and III) and 1.0232 x P_{c_n} (used for Phase II only).

(U) To determine the change in throat area during the firing of an ablative thrust chamber (Phases I and III), a calculated throat area, assuming c^*_{corr} as constant, was determined from

$$A_{T_{calc}} = \frac{c^*_{corr} \dot{W}_T}{P_{cc} g} \tag{4}$$

For the first firing of Phase I, c^*_{corr} was determined from Eq. (3) from 8.5 to 9.5 sec, and, for the first firing of Phase II, from 4.5 to 7.5 sec. These time periods were chosen to ensure that no significant throat area change had occurred. Since the value of c^*_{corr} should not

change appreciably during a firing, assuming the chamber pressure, mixture ratio, and total propellant flow rate remain constant, the calculated throat area obtained from Eq. (4) will indicate the change in throat area with time caused by ablation.

(U) The Phase II vacuum specific impulse data were corrected to adiabatic conditions by returning the heat lost to the cooling water. The resulting statement was:

$$(I_{sp})_1 = (I_{sp})_2 \left[\frac{h_o - (h_e)_1}{h_o - (h_e)_2 - \frac{\dot{Q}_W}{\dot{W}_W}} \right]^{1/2} \tag{5}$$

where

$( )_1$ = Adiabatic system

$( )_2$ = Water-cooled system

h_o = Stagnation enthalpy, Btu/lb_m

h_e = Exhaust gas enthalpy, Btu/lb_m

$\dot{Q}_W$ = Heat rejected to cooling water, Btu/sec

$\dot{W}_W$ = Flow rate of cooling water, lb_m/sec

A complete derivation of the above statement is contained in Appendix II of Ref. 2.

SECTION IV
RESULTS AND DISCUSSION

(U) This is a summary of the results of the four phases of altitude testing of the LEM Ascent Engine conducted in the Propulsion Engine Test Cell (J-2A). The engine configurations, firing sequence, firing durations, and pressure altitudes of each test are presented in Table I. It is the intention of this report to present the results of these four phases of testing as reported in Refs. 1 through 4 (see section 4.1). The results of the first phase of testing are compared with those of the third phase based on the information obtained from Phase II tests, which were conducted to determine the performance of the engine as a function of chamber pressure, mixture ratio, and chamber length (see section 4.2).

4.1 SUMMARY OF ENGINE PERFORMANCE

4.1.1 Vacuum Specific Impulse

(U) The results of the first three phases of testing lead to three distinct values of measured vacuum specific impulse. These values were influenced by (1) chamber pressure, (2) area ratio, (3) chamber length, and (4) cooling mechanism differences.

(C) Phase I testing incorporated two types of all-ablative, thrust-chamber-nozzle assemblies with an expansion ratio of 40:1 which were operated at 100-psia chamber pressure. Vacuum specific impulse (I_{sp_∞}) levels obtained 20 sec after initiation of the firings were (1) 308.9 lb_f-sec/lb_m for the AVCO assembly which incorporated the water-cooled thrust chamber extension (Test 01), (2) 307.0 lb_f-sec/lb_m for the HITCO assemblies which incorporated the water-cooled thrust-chamber extension (Tests 02 and 03), and (3) 305.4 lb_f-sec/lb_m for the HITCO assembly without the water-cooled assembly (Test 04). The AVCO assembly vacuum specific impulse increased throughout the 380-sec firing to a value of 310.9 lb_f-sec/lb_m. This value was attained just prior to the structural failure, which occurred after 263 sec of the 380-sec firing (see section 4.5). After the structural failure, which was the loss of a section of ablative material just downstream of the throat, the vacuum specific impulse dropped to a value of approximately 300.3 lb_f-sec/lb_m and rose to 302.0 lb_f-sec/lb_m just prior to the complete failure of the thrust-chamber-nozzle assembly at 378.2 sec. Vacuum specific impulse data from the remainder of the Phase I chambers were relatively constant throughout the 380-sec firings (Ref. 1).

(C) The Phase III engines, operating at approximately 120-psia chamber pressure and near 1.6 mixture ratio, attained a mean value of I_{sp_∞} of 309.3 lb_f-sec/lb_m. This value was reached approximately 20 sec after ignition. During the 380-sec firing the mean I_{sp_∞} attained was 309.5 lb_f-sec/lb_m. This value was attained by all three chambers with only minor differences (Ref. 3).

(U) Table II presents a tabulation of the data obtained during the first three phases of testing. These data represent the 20-sec data point for the Phase I and Phase III tests and the average of the last 10 sec of each firing for Phase II. Figure 7 presents the time histories of the vacuum specific impulse obtained from the ablative-chamber tests (Phases I and III).

(C) As seen in Fig. 7, the results of each firing of the Phase III test agree very well for the 380-sec firings in that the average vacuum specific

impulse remained relatively constant at 309.0 to 309.5 lb_f-sec/lb_m after the first 40 sec of the firings. The Phase I data for Runs 02 and 03 agree very well for the first 40 sec of the firings but then deviate. This deviation was caused by an increase in the mixture ratio (Ref. 1) from 1.60 to 1.76 during Test No. 02. The difference in chamber length effected by the removal of the water-cooled thrust chamber extension between Tests 03 and 04 had approximately the same effect on I_{sp_∞} as was experienced in Phase II.

(C) The all-metal, water-cooled, 45.6:1 area ratio assembly used during the second phase of testing attained I_{sp_∞} values of 305.8 and 303.3 lb_f-sec/lb_m, at mixture ratios of approximately 1.6 for chambers with and without the water-cooled combustion chamber extension, respectively. The average increase in I_{sp_∞} was approximately 0.78 percent due to the increased chamber length. These tests also indicated that the maximum value of vacuum specific impulse should occur at a mixture ratio of 1.6.

(C) Comparing Test 04 Phase I with the results of Phase III indicates that, for chambers of similar lengths, an increase in chamber pressure from 100 to 120 psia and an increase in area ratio from 40:1 to 45.6:1, the vacuum specific impulse increased approximately 1.25 percent.

4.1.2 Characteristic Velocity

(C) The characteristic velocity for an ablative chamber is a difficult parameter to determine. The fixed contour chamber tests conducted during Phase II of this program helped to determine the time at which steady-state operation was achieved during the ablative chamber tests. As seen in Fig. 8 which depicts a typical $P_c/\dot{W}_T$ variation with time (which is in effect the c* variation since A_T and g are constants), the value of $P_c/\dot{W}_T$ is essentially constant after about 2.5 sec. In all but two of the Phase II firings (total 28), the values of $Pc/\dot{W}_T$ were within ±0.25 percent of the steady-state value after 4.5 sec. The two firings that were not steady-state after 4.5 sec became stable after 10 to 15 sec.

(U) On the basis of the Phase II tests, the value of c* obtained after 4.5 sec during phases I and III should be representative values for the all-ablative assemblies because the propellant feed system should have stabilized and the throat area would not have changed significantly.

(U) Figure 9 presents c* data taken during Phases I, II, and III. The values for Phases I and III were taken at 4.5 sec, whereas the Phase II data were steady-state (an average of the last 10 sec of the firings). An increase in characteristic length (L*) of approximately

40 percent by the addition of the water-cooled thrust chamber extension resulted in an increase in c* for the Phase II tests of approximately 0.69 percent at a mixture ratio of 1.6. The Phase I c* data indicated that a similar change occurred for approximately the same change in chamber length. A change of injectors from a series A to a series B was also made at the time the chamber length was changed during the Phase I testing, but this had no effect on the resulting c*. The Phase I data are presented in Fig. 9 to show the relation of the data to that obtained during Phase II testing.

(U) The values of c* for the Phase II test calculated at 4.5 sec are also shown in Fig. 9. These values are exactly as reported in Ref. 3 and coincide somewhat with the Phase II results. As pointed out later in section 4.2.3, there is a discrepancy in the methods for arriving at a chamber pressure on which the performance of the engine is to be based. The values of c* do not compare very well when they are based on chamber pressure measured at similar positions in the chamber.

(C) The mean value of c* for the Phase III engine based on chamber pressure measured at the injector face and corrected as suggested by BAC (P_{cj} x 0.98621) was 5471 ft/sec at a mixture ratio near 1.6. For the all-metal chamber test, the maximum c* occurred at a mixture ratio of 1.5 (Ref. 2).

4.1.3 Nozzle Throat Area

(U) Variations in nozzle throat area are presented in Fig. 10 as a function of firing time for both the Phase I and the Phase III all-ablative, thrust-chamber-nozzle assemblies. These variations are presented in ratio form, as the ratio of calculated throat area (see section 3.2) to the pre-fire measured throat area.

(C) The Phase III assemblies decreased in throat area to an average value of 0.947 of the original areas after a total of 180 sec of firing time. The Phase I assemblies had decreased to only 0.975 at the same time. In general, the trend of the areas is similar for the chambers tested. The chambers tested during Phase III were exposed to higher heating rates than were those of Phase I because of the higher chamber pressures. However, no information was available as to the thermal properties of the ablative materials from which conclusions can be made concerning the effect of chamber pressure on ablation rate.

(C) The following is a comparison of the nozzle throat areas recorded throughout the program.

Phase	Test	Measured, in.^{2}		Final Calculated, in.^{2}	Percent Difference
		Pre-Fire	Post-Fire		
I	01	19.087	16.260	---	---†
I	02	19.221	19.470	---	---‡
I	03	19.213	18.704	18.720	+0.3
I	04	19.127	18.589	18.540	-0.3
III	C1	16.478	16.281	16.201	-0.5
III	C2	16.475	16.439	15.977	-2.8
III	C3	16.444	16.237	15.835	-2.5

† Structural failure made measurement impossible
‡ Large mixture ratio change during firing made calculations questionable.

The measured and calculated post-fire areas agree very well as shown above. It should be noted that the calculated area is actually the calculated aerodynamic area and is directly affected by such factors as the rate at which the ablation materials gasify, surface roughness, etc.

4.1.4 Vacuum Thrust Coefficient

(U) Calculated values for vacuum thrust coefficient (C_{F_∞}) as a function of mixture ratio are presented in Fig. 11 for Phases I, II, and III. It should be noted that the data for Phase II are different from those of Phases I and III, which were based on chamber pressures measured at a different location on the chamber. Phase II data were based on chamber static pressure measured at the nozzle entrance and were corrected to nozzle entrance total pressure by a factor supplied by BAC. Phases I and III data were based on chamber static pressure measured at the injector and were corrected by another factor supplied by BAC. These correction factors, which should give the same nozzle total pressure, yield different values of chamber total pressure at the nozzle entrance (see section 4.2.3), which resulted in two possible levels of C_{F_∞}.

(U) Results of the Phase II test indicated that in general (1) no increase in the thrust coefficient was experienced for variations in chamber pressure, (2) an increase in characteristic length of approximately 40 percent (from 30 to 42 in.) resulted in increases in C_{F_∞} from 0 to 0.56 percent for a mixture ratio range from 1.4 to 2.0, and (3) C_{F_∞} increased with increased mixture ratio.

4.1.5 Simulated Stage-Separation Test

(U) Eighteen 650-msec firings of the LEM Ascent engine were conducted to evaluate the effects of staging at near vacuum conditions (Phase IV, Ref. 4). A movable flat plate was installed near the nozzle exit plane to simulate the Descent Stage blast shield (Fig. 5b).

(U) The presence of the flat plate induced a shock in the nozzle as long as the plate was positioned 7 in. or less from the nozzle exit. The angular movement of the plate had no apparent effect on the location of the shock until the plate was 7 in. from the exit and the angle was increased to 10 deg; then the shock moved out of the nozzle completely. When the blast shield was positioned 10 in. from the exit plane the shock had moved completely out of the nozzle regardless of the plate angle. Figure 12 indicates the approximate location of the shock patterns within the limits of the instrumentation available. The crosshatched area indicates that the shock was present somewhere between two pressure taps and also indicates the relationship of the location of the blast shield relative to the shock location. Table III indicates the nozzle static pressure levels that were experienced during this phase of testing. Reference 4 indicated that the cell pressure at the start of each run was approximately 0.25 psia and increased to approximately 0.80 psia at the end of each 650-msec firing. The ratio of the cell pressure to the nozzle exit static pressure (actually the tap located at area ratio of 41.4) was approximately 0.15. This ratio is sufficient to simulate space conditions very closely since further reductions in ambient pressure would have no effect on the general flow pattern except to strengthen the shock pattern outside of the nozzle. Figure 13 presents the variation of thrust with respect to blast shield location.

(U) The results of this free-jet test demonstrated that the LEM Ascent engine can withstand the momentary loads and unsymmetrical forces which may occur during lunar liftoff.

4.2 PERFORMANCE CORRELATION

(C) Several different configurations of the LEM Ascent engine were tested during this program (Table I). In order to compare performance, it was necessary to reference the performance parameters to a common configuration and to common operating conditions. The following final flight configuration and design operating conditions were chosen as the common reference:

Chamber: HITCO Ablative, H - (X) - 350.3, L* = 30 in.
Injector: B3-L2
Nozzle: A/A_T = 45.6, Throat Area (nominal) = 16.44 $in.^2$

Operating Conditions:

a. Mixture Ratio = 1.6
b. Chamber Pressure Measured at the Injector Face = 120 psia

Because of the changing geometry of the ablative engines, two distinct time slices were chosen for investigation: (1) Four and one-half seconds[1] after the firing signal was selected as the first time slice since by this time chamber pressure, mixture ratio, and total propellant flow had become stable and nozzle throat ablation should scarcely have begun (Ref. 3); (2) twenty seconds after the firing signal was selected as the second time slice as it fell within the operating period of the largest number of samples. Only data from firings at a nominal mixture ratio of 1.6 and, for the Phase II firings, only data at a nominal chamber pressure of 120 psia and the design L* of 30 in. were considered. This selection of data was deemed advisable since it provided a comparable number of samples from each phase with a minimum amount of data adjustment.

(U) A limited amount of data from the 0.650-sec firings of Phase IV is presented for comparison. These data were averaged over the last 0.3 sec prior to the engine shutdown signal.

4.2.1 Data Adjustment (4.5 sec)

4.2.1.1 Phase I

(C) The Phase I performance parameters at 4.5 sec are presented in columns 1 through 11 in Table IV. These values are as measured or calculated in Ref. 1 and include no adjustments to the reference conditions. (Data from test 01-01 were omitted because of a high mixture ratio.) The Phase I performance data are not compatible with the reference standard conditions because:

1. Injectors used were A3 - (X) and B3 - (X) types,
2. The nozzle had a 40:1 expansion ratio and a 19.20 $in.^2$ nominal throat area,
3. Nominal chamber pressure was 100 psia, and
4. The first two engines utilized a 4.125-in.-diam, water-cooled section in the thrust chamber

---

[1] Data were averaged for one-half second before and after the specified time.

Because of this incompatibility, adjustment of the Phase I data to the reference standard is required to facilitate data comparisons. No adjustment to the performance data was made to account for the use of injectors other than the standard as examination of the measured data revealed no detectable difference in performance. Adjustment of vacuum specific impulse to account for a nonstandard area ratio nozzle was made as follows:

$$I_{sp_A} = I_{sp} \left(\frac{I_{sp}\ 46.5}{I_{sp}\ 40.0} \right)$$

where the theoretical values of specific impulse at area ratios of 40 and 46.5 were taken from Ref. 9. The adjustment of performance data to a chamber pressure of 120 psia was made using the results of data analysis from the Phase II hard contour tests. It was found that specific impulse increased 0.766 percent for an increase in chamber pressure from 100 to 120 psia (Ref. 2). Therefore, the second adjustment applied to the first gives

$$I_{sp_B} = I_{sp_A} (1.00766) \frac{(120 - p_{cc_i})}{20}$$

(U) It should be pointed out that this adjustment assumes, first, that the chamber pressure varies as a function of propellant flow identically for both engines (i. e., the slope of the $P_c/\dot{W}_T$ curve is the same for both engines). Actually, since the throat area of the Phase I engines was larger than the Phase II engines it would be expected that the slope of the $P_c/\dot{W}_T$ curve for the Phase I engine would be less than that of the Phase II engines. Secondly, it is assumed, in making this adjustment, that the $P_c/\dot{W}_T$ curve remains linear between 100 and 120 psia even though the engine is operating 20 percent above design chamber pressure. Therefore, the values of I_{sp_B} adjusted to a chamber pressure of 120 psia are probably optimistic. It was necessary to make a third adjustment to the specific impulse values of Phase I firings 02-01 and 03-01 to account for the difference in L* from standard. Phase II tests also showed that the addition of a 4.125-in.-diam water-cooled section in the thrust chamber increased vacuum specific impulse by 0.78 percent at a mixture ratio of 1.6. Therefore, the third adjustment applied to the second gives

$$I_{sp_{adj}} = I_{sp_B} (0.9922)$$

The final adjusted values of vacuum specific impulse are presented in column 13 of Table IV.

4.2.1.2 Phase II

(U) Phase II performance parameters at 4.5 sec are presented in columns 1 through 11 in Table IV. These values are as measured or

calculated in Ref. 2 and include no adjustments to the reference standard conditions. Those calculations involving chamber pressure have been carried out using two different measurements: one taken at the nozzle entrance (P_{cc_n}) and another taken at the injector face (P_{cc_i}). A more detailed discussion of the chamber pressure measured at the two locations is included in section 4.2.2. As previously discussed, only selected data are shown. These data are not compatible with the reference standard because:

1. A hard contour, water-cooled thrust chamber was used,
2. Injectors were of the B3-L2 and B3-(X) types, and
3. Chamber pressures were other than the standard.

An adjustment was made to the Phase II vacuum specific impulse values to account for heat loss to the chamber cooling water. This adjustment, which is described in Ref. 2, estimates the performance of an identical, but adiabatic, chamber. No adjustment was made to account for the use of two different injectors as examination of the data revealed no difference in performance. Specific impulse was adjusted to a 120-psi chamber pressure reference by extrapolating along the $P_{cc_i}/\dot{W}_T$ curve obtained from Phase II survey data. Column 13 in Table IV shows adjusted vacuum specific impulses. The other adjusted performance parameters presented in columns 12 through 15 were calculated from adjusted specific impulse using the basic relationships.

4.2.1.3 Phase III

(U) Phase III performance parameters at 4.5 sec are presented in columns 1 through 11 in Table IV. These values are as measured or calculated in Ref. 3 and include no adjustments to the reference standard conditions. Performance parameters have been included in columns 12 through 15, which include minor chamber pressure adjustments to the 120-psia standard. The method of adjustment was identical to that used for Phase II data.

4.2.1.4 Phase IV

(U) Phase IV performance parameters averaged over the final 0.3 sec prior to termination of the 650-msec firings have been presented in columns 1 through 11 in Table IV. Only firings 15 through 18 have been included because these data were unaffected by the plate at the nozzle exit (Ref. 4). Propellant flow data were not obtained for these tests; therefore, the performance parameters dependent upon total fuel flow rate were not included.

4.2.2 Data Adjustment (20 sec)

(U) Performance parameters for Phases I, II, and III at 20 sec are presented in Table IV. The methods of adjustment were identical to those used for the 4.5-sec data. The sample selection varies somewhat between Tables IV and V because of the time slice chosen. The 20-sec data for Phase III, firings C1-02, C2-02, and C3-02, were taken, as before, 20 sec after the firing signal but represent 80 sec of total time on each of the three engines.

(U) Performance parameters listed to the right of the heavy vertical lines in Tables IV and V are adjusted values, and the data from different phases are now considered comparable.

4.2.3 Chamber Pressure

(U) The values of characteristic velocity and thrust coefficient presented in Ref. 2 for the Phase II firings were calculated using a chamber static pressure measurement taken at the nozzle throat entrance. This pressure was multiplied by a factor (1.0232) supplied by BAC to refer the pressure to a total pressure value at the nozzle entrance plane (P_{cc_n}). The pressures used for performance calculations for Phases I, III, and IV firings were measured at the injector face, and a BAC supplied adjustment factor (0.98621) was applied to refer the pressure to a total value at the same location (P_{cc_i}). For Phase II firings, chamber pressure was measured at both the injector face and nozzle throat entrance. A comparison of the chamber pressures measured at the two different locations with the appropriate correction factor applied revealed the following:

1. There was a general disagreement as to the actual value of chamber pressure at the nozzle entrance plane.
2. The difference between P_{cc_i} and P_{cc_n} data for the same firing is as much as 2.4 psia. The P_{cc_n} values averaged 1.48 psia higher than the P_{cc_i} data at a nominal mixture ratio of 1.6.
3. The pressure measured at the nozzle entrance plane (P_{cc_n}) was more consistent and linear with respect to total propellant flow ($\dot{W}_T$) than was the pressure measured at the injector face (P_{cc_i})

From these observations, it is evident that for proper separate evaluation of the components (i.e., injectors, chamber, and nozzle) and ultimate optimization of the engine, further study must dictate the optimum location for chamber pressure measurement and appropriate correction factors. Even though the P_{cc_i} data exhibit more scatter than the P_{cc_n}

data, chamber pressure measured at a location common to all series (P_{cc_i}) should be used for comparing all calculated performance data involving chamber pressure. Values of P_{cc_i} and P_{cc_n} are presented in columns 4 and 5 of Table IV for comparison. Also presented is a value of P_{cc_i} adjusted to an adiabatic chamber ($P_{cc_{i_A}}$). This value of chamber pressure, presented in column 16, was calculated from vacuum specific impulse adjusted to adiabatic conditions assuming that the thrust coefficient is independent of chamber pressure.†

(U) The values of chamber pressure in columns 4 and 5 are shown as functions of total propellant flow rate in Fig. 14. Values are also shown from four additional Phase II firings at nominal chamber pressures of 100 and 140 psia in order to better establish the slope of the curve. It is seen that the Phase II and Phase III P_{cc_i} data compare favorably at this time slice, whereas the P_{cc_n} data of Phase II appear to be slightly higher. This agreement of Phase II and III P_{cc_i} data should be interpreted only as comparable performance of the hard-contour and ablative engines while both engines were still geometrically identical. The agreement should not be considered as a basis for assuming that the P_{cc_i} data are more accurate than the P_{cc_n} data.

(U) Chamber pressure as a function of flow rate is shown in Fig. 15 for the 20-sec data in Table V. The effect of nozzle throat area change is shown here by the inclusion of lines of various throat areas; these were calculated by the techniques of Refs. 1 and 3, assuming a constant characteristic velocity early in the firing when ablation would be expected to have a negligible effect on performance.

4.2.4 Vacuum Specific Impulse

(U) The values of vacuum specific impulse at 4.5 sec, both measured and adjusted, are shown as functions of mixture ratio in Fig. 16. It is seen that the adjusted values from Phases I, II, and III compare favorably. Even though the individual specific impulse values for the three phases appear to be within the overall accuracy of the data, the average of the Phase III points is approximately one second higher than that of Phase II. If the adiabatic adjustment of Phase II data actually restored all lost heat to the combustion products, then the performance of the hard-contour, Phase II engine with smooth chamber and nozzle

---

†Examination of Phase II measured data revealed that a change in C_{F_∞} of less than 0.2 percent occurred for a 40-psia change in chamber pressure.

walls would be expected to be at least as high as the Phase III ablative chambers. This apparent discrepancy must be attributed to one, or both, of the following:

1. The adiabatic adjustment simulated restoration of the heat rejected to the chamber and nozzle throat cooling water only. All other possible heat losses were neglected, which means that the adjustment was minimal.
2. It was assumed that no ablation had occurred at 4.5 sec, and therefore, the Phase III chambers should have been identical, dimensionally, with the Phase II chambers. This assumption may be in slight error.

(U) The values of vacuum specific impulse at 20 sec, both measured and adjusted, are shown as functions of mixture ratio in Fig. 17. The three additional Phase III data points are from the second firings of the three engines tested. Comparing phase data here shows the effect of the decreasing throat area already seen in Fig. 15 as an increase in the $P_{cc_i}/\dot{W}_T$ ratio. The apparent performance increase with a decreasing throat area is thought to be the same phenomenon as was found in the Phase II hard-contour tests when the 4.125-in.-diam, water-cooled section was added to the thrust chamber. It was shown in Refs. 1 and 2 that an increase in characteristic length (L*) caused an increase in performance, presumably because the thrust chamber was designed with a less than optimum L*. Reducing the nozzle throat area while holding the chamber volume constant † (Phase III) would have the same theoretical effect on combustion efficiency as holding the nozzle throat area constant and increasing chamber volume (Phase II), provided total propellant flow is reduced in proportion to throat area in the former case.

(U) Average adjusted performance parameters at 4.5 and 20 sec are shown in Fig. 18 for Phases II and III. It is seen that the total propellant flow rate does decrease with throat area as chamber pressure remains relatively constant for the Phase III firings. The decreasing propellant flow rate is the result of a decreasing propellant system supply pressure. A very elementary approach to the idea of increasing performance with decreasing throat area is that the ablating engine with

---

† Actually the chamber volume should increase slightly during the ablation process, which further increases the chamber volume with respect to throat area.

reduced throat area can be considered as a smaller engine with a slightly larger A_e/A_T operating at a higher combustion efficiency than a non-ablating (or hard-contour) engine. Although specific impulse is higher for the ablating engine, throat area, flow rate, and thrust are lower while chamber pressure is approximately the same. Although the throat area at 20 sec is a calculated value based on the assumption of a constant characteristic velocity, it is supported by a calculated value assuming a constant thrust coefficient taken at 4.5 sec. The two average values of nozzle throat area thus calculated were 16.05 and 16.10 in.^{2}, respectively, or a disagreement of 0.3 percent. The thrust coefficient for the Phase III data increased slightly between 4.5 and 20 sec (column 14 in Table IV and column 11 in Table V) which was presumably caused by the increasing A_e/A_T ratio as the throat area decreased.

(U) Although no propellant flow rate data are available for Phase IV firings and, therefore, firm conclusions cannot be drawn concerning performance, it is interesting to note the similarity in Phase II and IV average chamber pressure, thrust, and thrust coefficient (columns 16, 17, and 18 in Table IV). Post-test examination of the Phase IV engine revealed no ablation; therefore, Phase II and IV engine dimensions were identical within manufacturing tolerances. The propellant supply pressure data of Phase III were used to set propellant supply tank pressures for Phase IV; therefore, mixture ratio and total flow should be approximately nominal.

(U) It was concluded that the performance of the ablative and the hard-contour engines was comparable when all data were referenced to the same standard. The apparent higher performance level of the ablative engines over the hard-contour engine was attributed to increased combustion efficiency as a result of a decreasing throat area.

4.3 ABLATION CHARACTERISTICS

(C) The mass ablation rates presented in the table on the following page were defined as the total loss in mass of the engine divided by the total burn time of the engine. The mass loss was determined from the pre-fire and post-fire weight measurements.

Phase	Test	P_c, psia	Assembly Weight, lb_m		Burn Time, sec	Mass Ablation Rate, lb_m/sec
			Pre-Fire	Post-Fire		
I	01	100	145.56	---	388	Structural Failure
I	02	100	137.88	125.88	397	0.03037
I	03	100	154.94	143.50	398	0.02896
I	04	100	161.63	150.75	395	0.02753
III	C1	120	145.50	133.0 †	445	0.02808 †
III	C2	120	146.00	128.19	445	0.04003
III	C3	120	144.28	129.69	444	0.03265

† This chamber was initially post-test weighed at 139.31 lb and was later reweighed at 133.0 lb by BAC.

(C) The average ablation rate of the Phase I thrust-chamber-nozzle assemblies was 0.02895 lb_m/sec, and the Phase III average was 0.03358 lb_m/sec. These two rates differ by approximately 14 percent. The Phase III tests were conducted at 120-psia and the Phase I at 100-psia chamber pressures. This variation in chamber pressure should give approximately a 15-percent increase in the convective heating rate resulting in the increased ablation rate.

4.4 ENGINE TEMPERATURES

(U) The maximum temperatures experienced on the external surface of the all-ablative, thrust-chamber-nozzle assemblies agree very well (Fig. 19). The maximum variation at any given station on these assemblies was less than 70°F throughout the program except for test C2 of Phase III. This particular test was conducted with minimum time between the 60- and 380-sec firings and without any maximum limitation being placed on the external temperature prior to firing. This resulted in the external temperature of the chamber being about 75°F higher than the other chamber temperatures at the start of the 380-sec firing. The maximum temperatures indicated in Fig. 19 occurred during the one-hour coast periods after the 380-sec firings (see section 3.1).

(U) The maximum external temperatures near the throats of the chambers tested during Phase I were somewhat lower than those indicated during Phase III. This was expected because of the thicker ablator and insulator layers on these chambers in the throat area (Fig. 2) and because of a lower operating chamber pressure.

(C) In general, the maximum external temperature rise that should be expected for similar chambers and firing durations of 380 sec should be approximately 400°F and would occur along the thrust chamber wall.

4.5 ENGINE STRUCTURAL INTEGRITY

(C) The four phases of this test program were conducted with only one major structural failure. The first test period of Phase I, using an AVCO chamber, resulted in the chamber failing completely after 378 sec of an expected 380-sec test. A portion of the ablative material just downstream of the throat separated from the engine after 263 sec of the 380-sec firing. The loss of this section of ablative material allowed the hot gases to enter the insulation layer (Fig. 2a) and eventually caused the failure of the thrust chamber section (Ref. 1). At the time of failure the thrust-chamber-nozzle assembly had a total firing time of 388 sec of an expected 455-sec life.

(U) The remainder of the ablative assemblies utilized in this program were HITCO assemblies. These seven assemblies experienced only minor structural degradation. The assembly used for Test C3 of Phase III was found to have a circumferential crack approximately 0.2 in. wide in the throat section (Fig. 20). The depth of the crack was not determined at AEDC. Post-fire inspection of all seven HITCO assemblies revealed that grooving along the chamber walls and rather extensive shingling or separation of the material layers in the nozzle downstream of the throat had occurred (Figs. 21 and 22). There was also some evidence of separation of the ablative material downstream of the throat from the structural wrap (Fig. 21) (Refs. 2 and 3).

(U) The destructive inspection required to determine the extent of separations of material, depth of char, material strength, etc., was not accomplished at AEDC. All chambers were returned to BAC for this type of inspection.

SECTION V
SUMMARY OF RESULTS

(U) The results of the simulated altitude testing of the BAC Model 8258 LEM Ascent engine in the Propulsion Engine Test Cell (J-2A) were as follows:

(C) 1. The mean values of vacuum specific impulse for the Phase I and III engines were 305.4 and 309.5 lb_f-sec/lb_m, respectively. These values compare very well when adjusted for

variations in chamber pressure, chamber length, and heat loss (based on Phase II test data) and for differences in expansion ratio (based on theory).

(C) 2. Initial performance evaluation (4.5-sec data) indicated that the characteristic velocity and vacuum thrust coefficient for the Phase I engine were 5510 ft/sec and 1.774, respectively. The Phase III engine performance indicated that c* and C_{F_∞} levels of 5468 ft/sec and 1.808, respectively, were obtained.

(C) 3. The Phase II all-metal engine performance indicated:

a. The effect of increasing chamber pressure 20 percent (from 100 to 120 psia) was to increase c* 0.766 percent and I_{sp_∞} 0.766 percent. No increase in C_{F_∞} was obtained.

b. The effect of increasing L* by 40 percent (from 30 to 42 in.) resulted in average increases of c* and I_{sp_∞} of 0.69 and 0.78 percent, respectively. The maximum increase in vacuum thrust coefficient was 0.56 percent, which occurred at a mixture ratio of 2.0.

c. The maximum value of c* was reached at a mixture ratio of 1.5, and the maximum I_{sp_∞} was reached at 1.6 for all configurations. Increasing mixture ratio increased C_F throughout the range tested.

(C) 4. The average mass ablation rates for the Phase I and III engines were 0.0290 and 0.0336 lb_m/sec, respectively.

(C) 5. The maximum external surface temperature rise on the all-ablative assemblies should be less than 400°F for a 380-sec firing.

(U) 6. The Phase I thrust-chamber-nozzle assembly built by AVCO did not meet the expected life requirements of 455 sec because it failed during Phase I Test No. 01 after a total firing time of 388 sec. The remainder of the chambers tested during Phase I experienced only minor structural degradation. The chambers tested during test Phases III and IV were structurally capable of meeting the requirements of the mission duty cycle and the proposed staging technique for the LEM vehicle.

REFERENCES

1. Barebo, R. L. and Matkins, E. H. (U) "Altitude Development Tests of the Bell Model 8258 Liquid-Propellant Rocket Engine, Phase I, LEM Ascent Stage Primary Propulsion System." AEDC-TDR-64-211 (AD355167), November 1964. (Confidential)

2. Ansley, R. C., Farrow, K. L., and Harper, C. W. (U) "An Altitude Performance Survey of a Water-Cooled BAC Model 8258 Rocket Engine at Various Chamber Pressures and Mixture Ratios, Phase II, LEM Ascent Stage Primary Propulsion System." AEDC-TDR-64-258 (AD355848), December 1964. (Confidential)

3. Ward, T. R. and Matkins, E. H. (U) "Altitude Development Tests of the Phase C Bell Model 8258 Liquid-Propellant Rocket Engine, Phase III, LEM Ascent Stage Primary Propulsion System." AEDC-TDR-64-242 (AD355847), November 1964. (Confidential)

4. Ward, T. R. and Palmer, W. T. (U) "The Effects of a Simulated Stage Separation Test on the LEM Ascent Engine, Phase IV, LEM Ascent Stage Primary Propulsion System." AEDC-TR-65-2 (AD356709), January 1965. (Confidential)

5. BAC LEM Ascent Engine (Model 8258). (U) "Nozzle Extension Development Test." (AEDC Test Plan) BAC Report No. 8258-927003, March 23, 1964. (Confidential)

6. Test Facilities Handbook, (5th Edition). "Rocket Test Facility, Volume 2." Arnold Engineering Development Center, July 1963.

7. Harper, C. W. "An Analysis of the Accuracy of Liquid-Propellant Rocket Engine Performance Measurements in the Propulsion Engine Test Cell (J-2A)." AEDC-TR-65-51 (AD460563), April 1965.

8. Minzner, R. A., Champion, K. S. W., and Pond, H. L. "The ARDC Model Atmosphere 1959." AFCRC-TR-59-267, August 1959.

9. Goldford, A. and Haupt, C. "Theoretical Performance of Nitrogen Tetroxide-Aerozine 50 Propellant System." Grumman Aircraft Engineering Corp., Report No. LED-271-2, August 20, 1963.

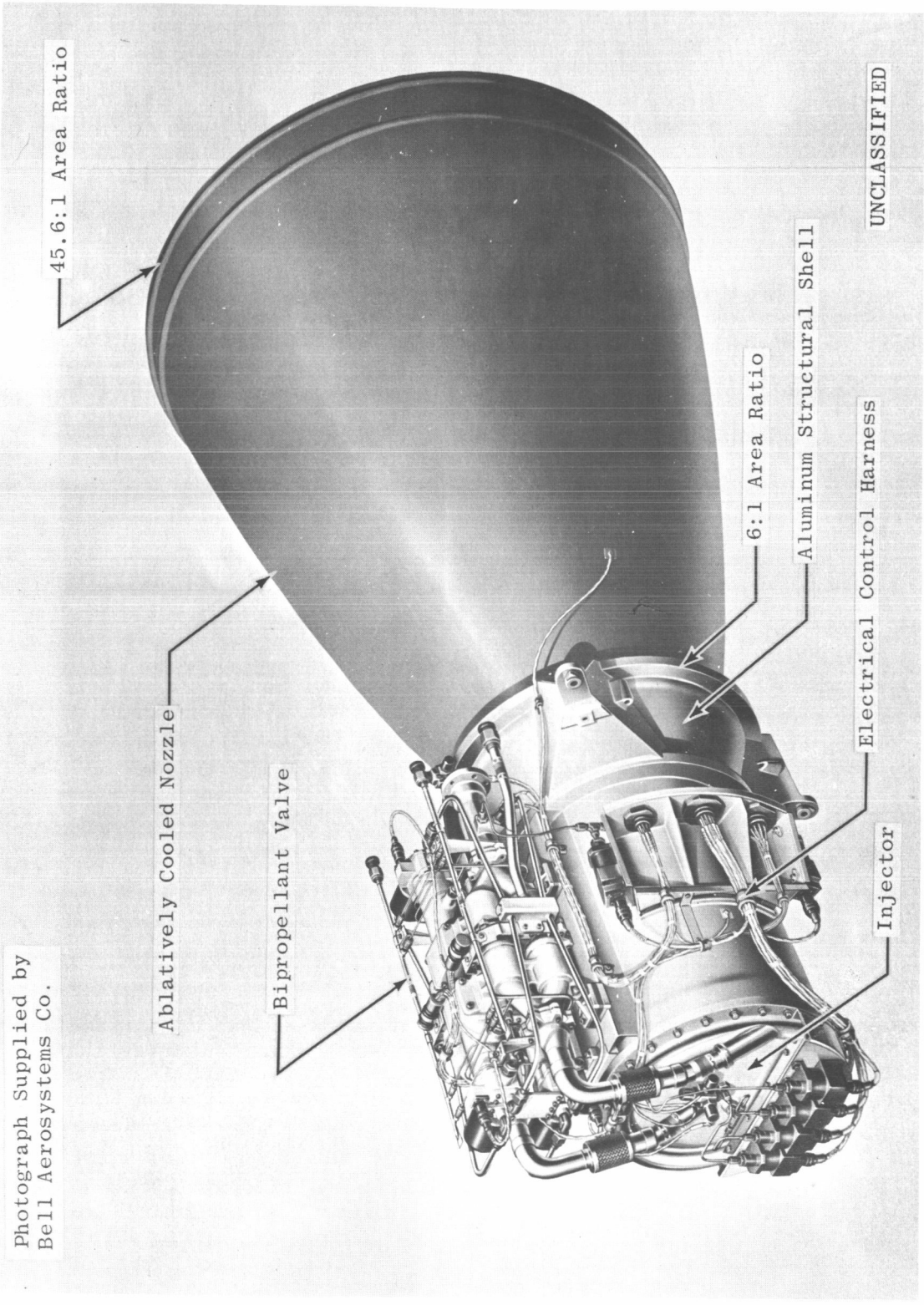

Fig. 1 LEM Ascent Engine

Station	Ablator Thickness, in.	Insulator Thickness, in.	Structural Wrap Thickness, in.
4.0	0.76	0.65	0.09
10.07	1.32	0.75	0.09
13.42	1.10	0.75	0.09
15.20	0.95	0.70	0.09
29.40	0.70	----	0.09
43.00	0.57	----	0.09

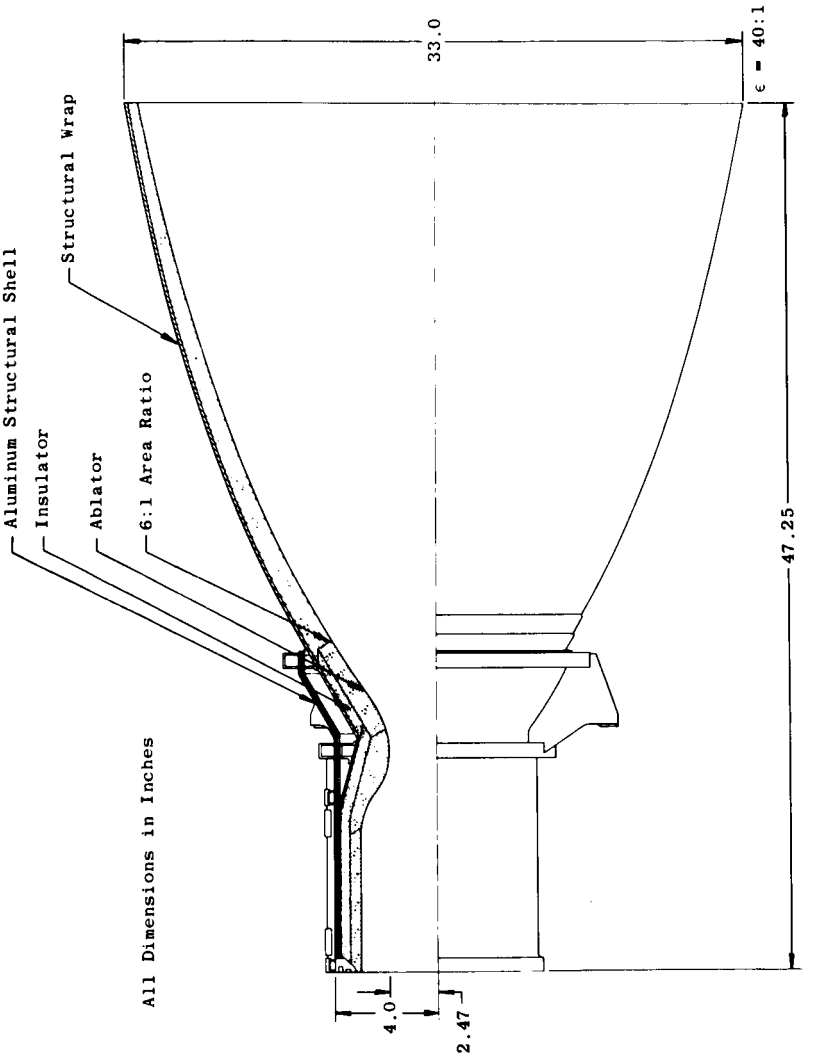

a. AVCO Assembly, Phase I

Fig. 2 Cross Section of Thrust-Chamber-Nozzle Assemblies

Station	Ablator Thickness, in.	Insulator Thickness, in.	Structural Wrap Thickness, in.
3.96	0.76	0.50	0.09
10.40	0.92	0.47	0.06
11.50	0.92	0.48	0.38
13.90	0.81	0.49	0.30
16.90	1.03	----	0.12
22.60	0.97	----	0.10
28.01	0.87	----	0.10
35.15	0.74	----	0.10
40.997	0.69	----	0.08

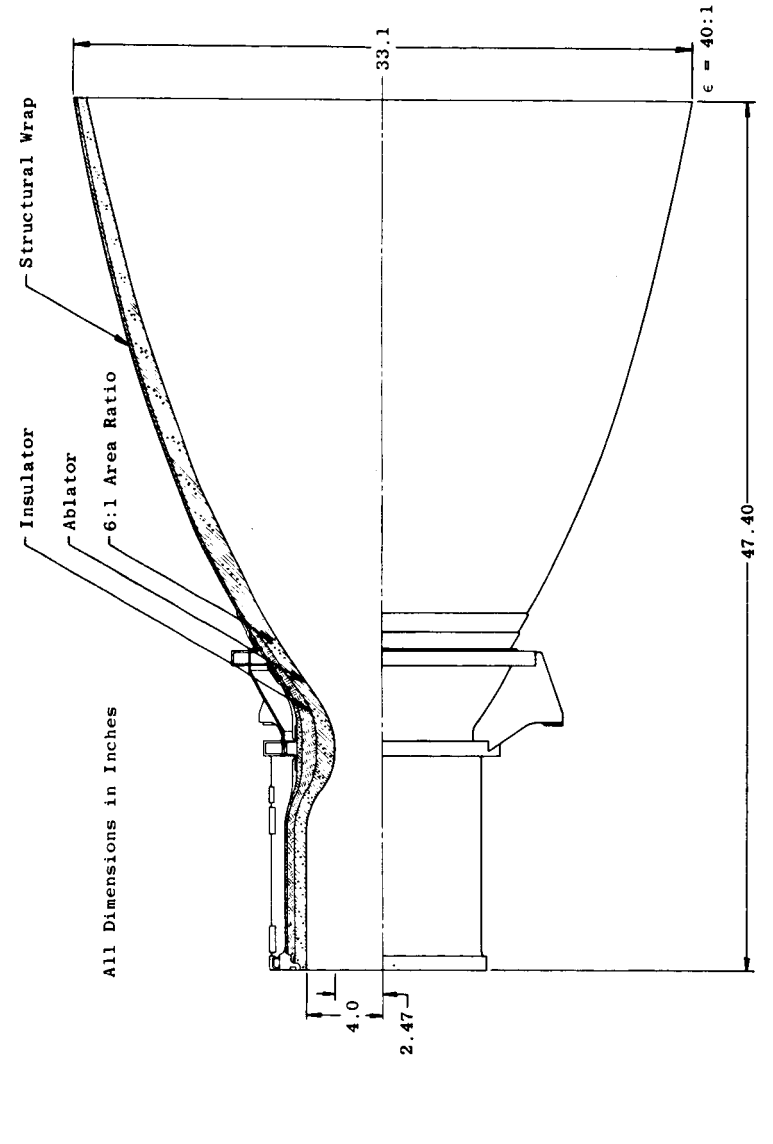

b. HITCO No. 1, Phase I

Fig. 2 Continued

UNCLASSIFIED

Station	Ablator Thickness, in.	Insulator Thickness, in.	Structural Wrap Thickness, in.
3.96	0.76	0.50	0.09
10.40	0.92	0.47	0.06
11.50	0.92	0.48	0.38
13.90	0.81	0.49	0.30
16.90	0.50	0.53	0.12
28.01	0.40	0.47	0.10
40.997	0.30	0.39	0.08

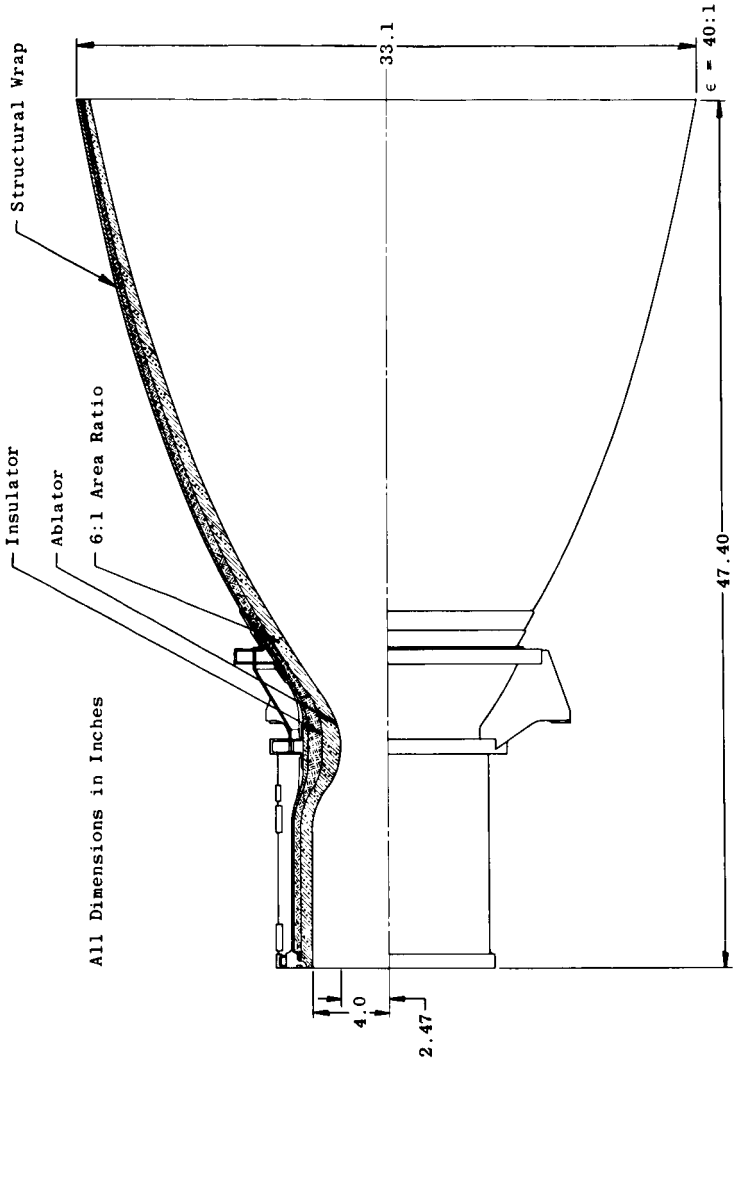

c. HITCO No. 2 and No. 3, Phase I

Fig. 2 Continued

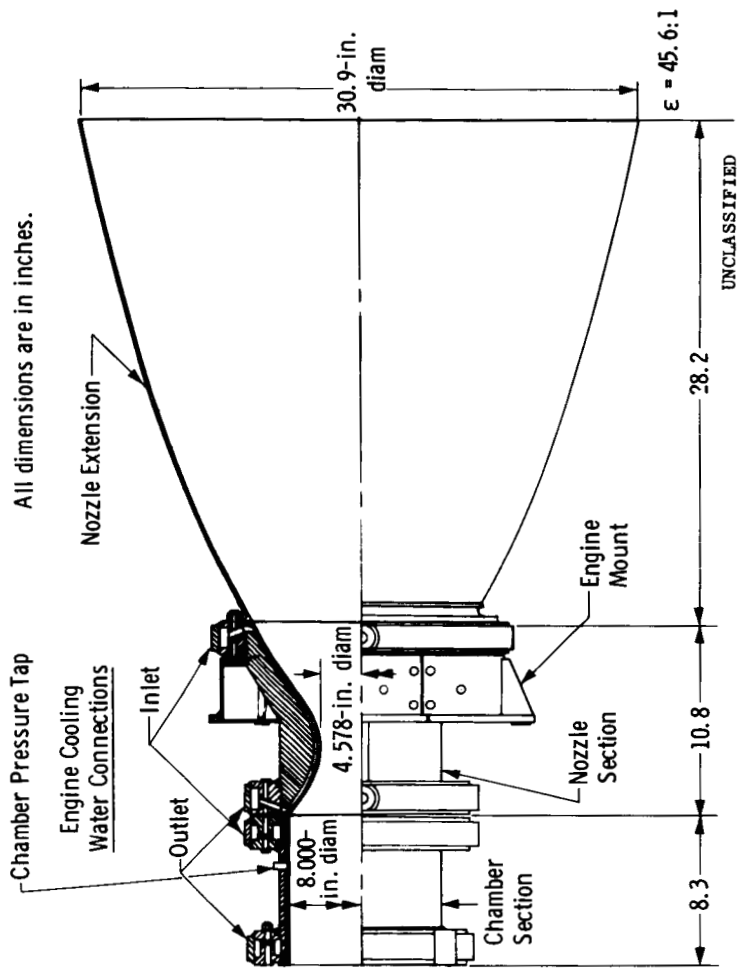

d. Water-Cooled Assembly, Phase II

Fig. 2 Continued

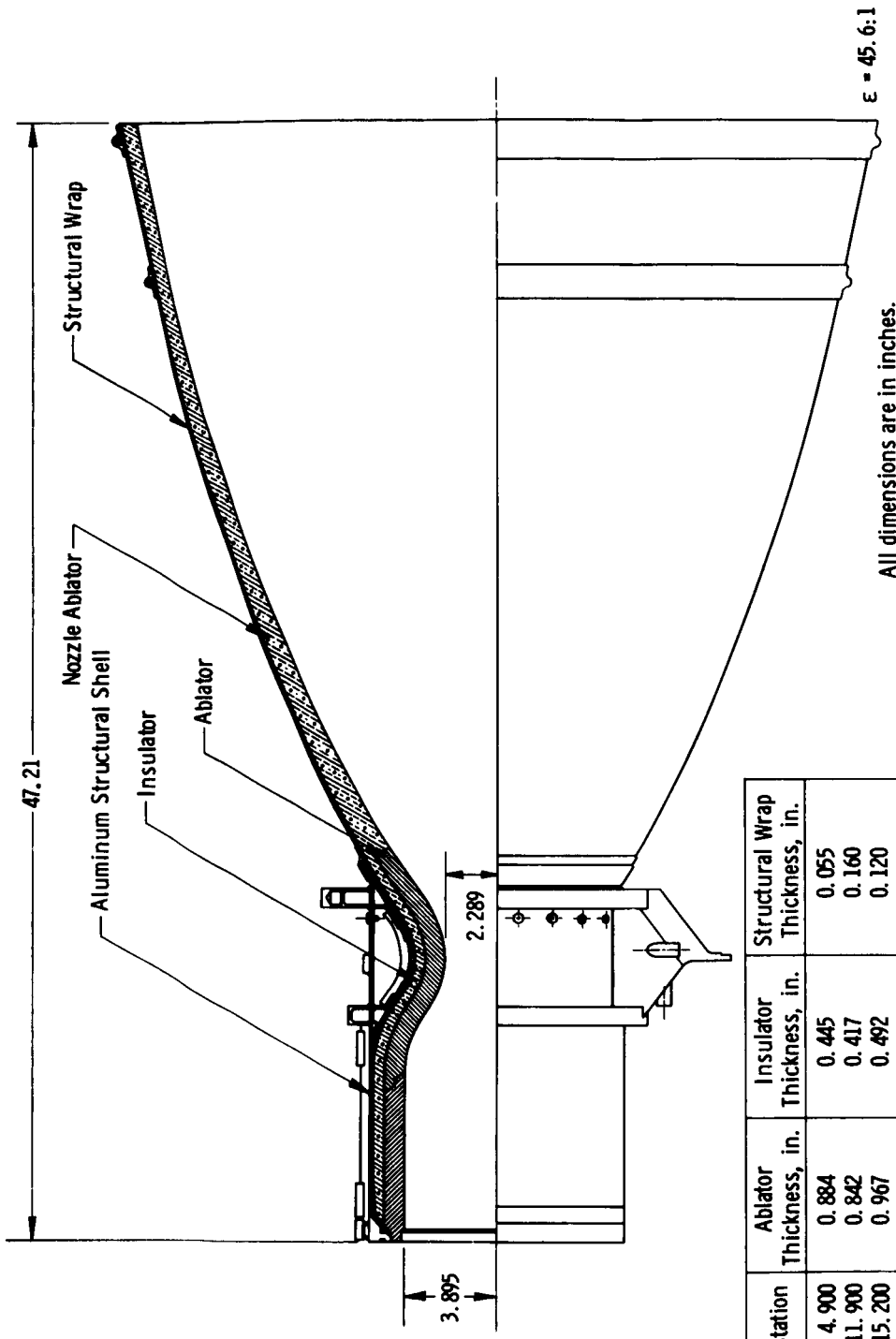

Station	Ablator Thickness, in.	Insulator Thickness, in.	Structural Wrap Thickness, in.
4.900	0.884	0.445	0.055
11.900	0.842	0.417	0.160
15.200	0.967	0.492	0.120
22.440	0.999	-----	0.097
32.377	0.755	-----	0.068
47.210	0.585	-----	0.051

e. HITCO Assembly, Phases III and IV

Fig. 2 Concluded

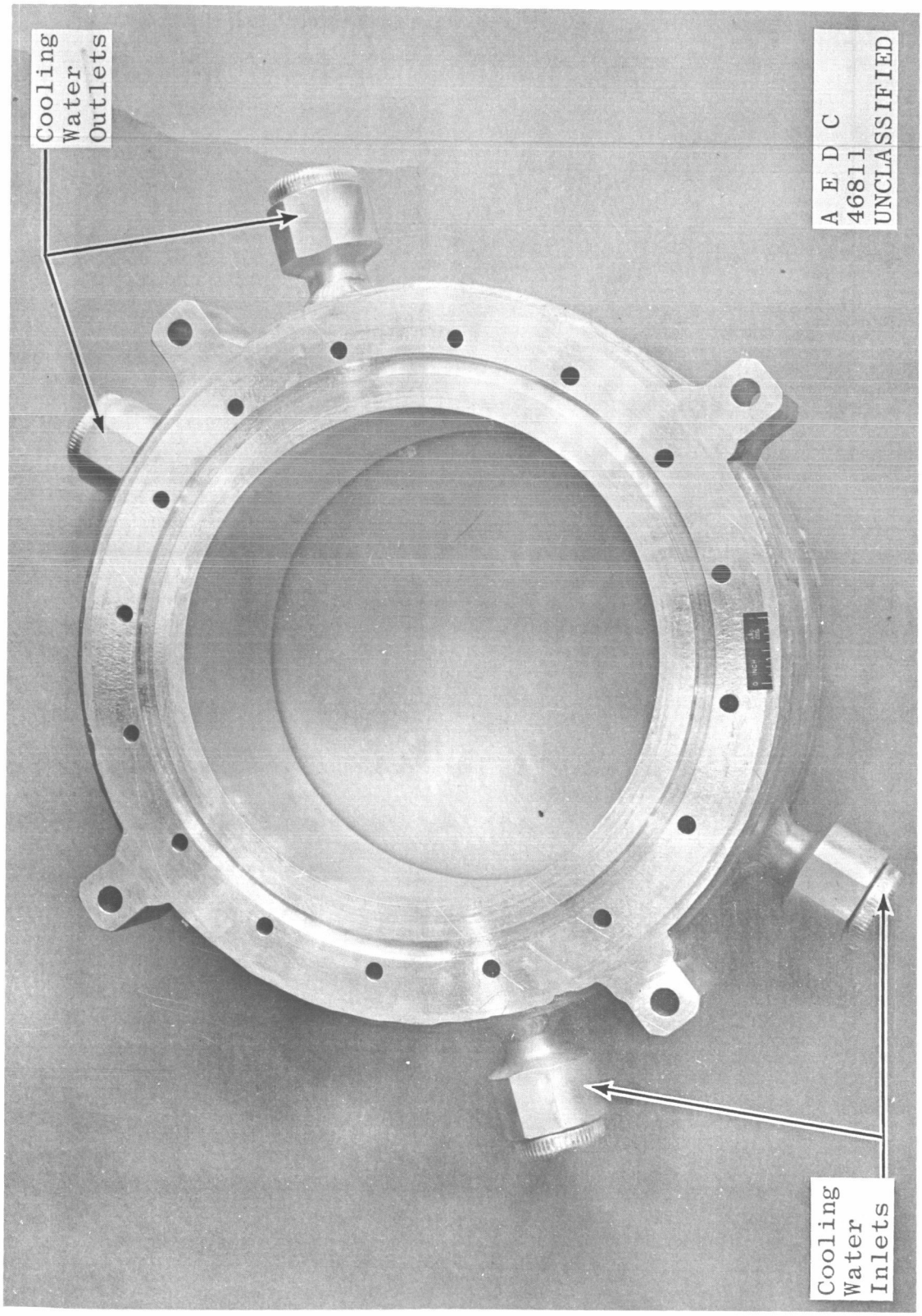

Fig. 3 Water-Cooled Thrust Chamber Extension

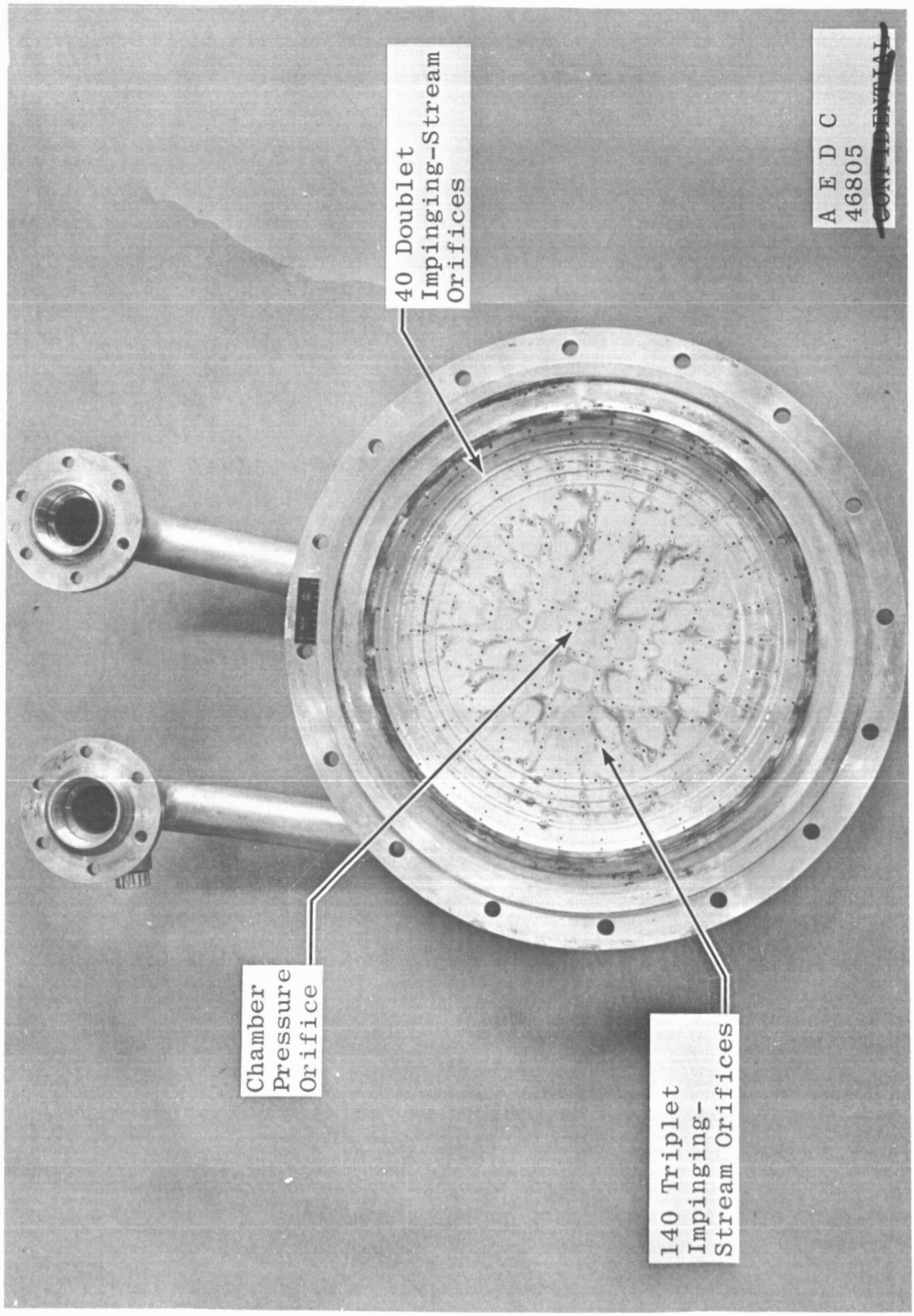

a. Series A

Fig. 4 LEM Ascent Engine Injector Assemblies

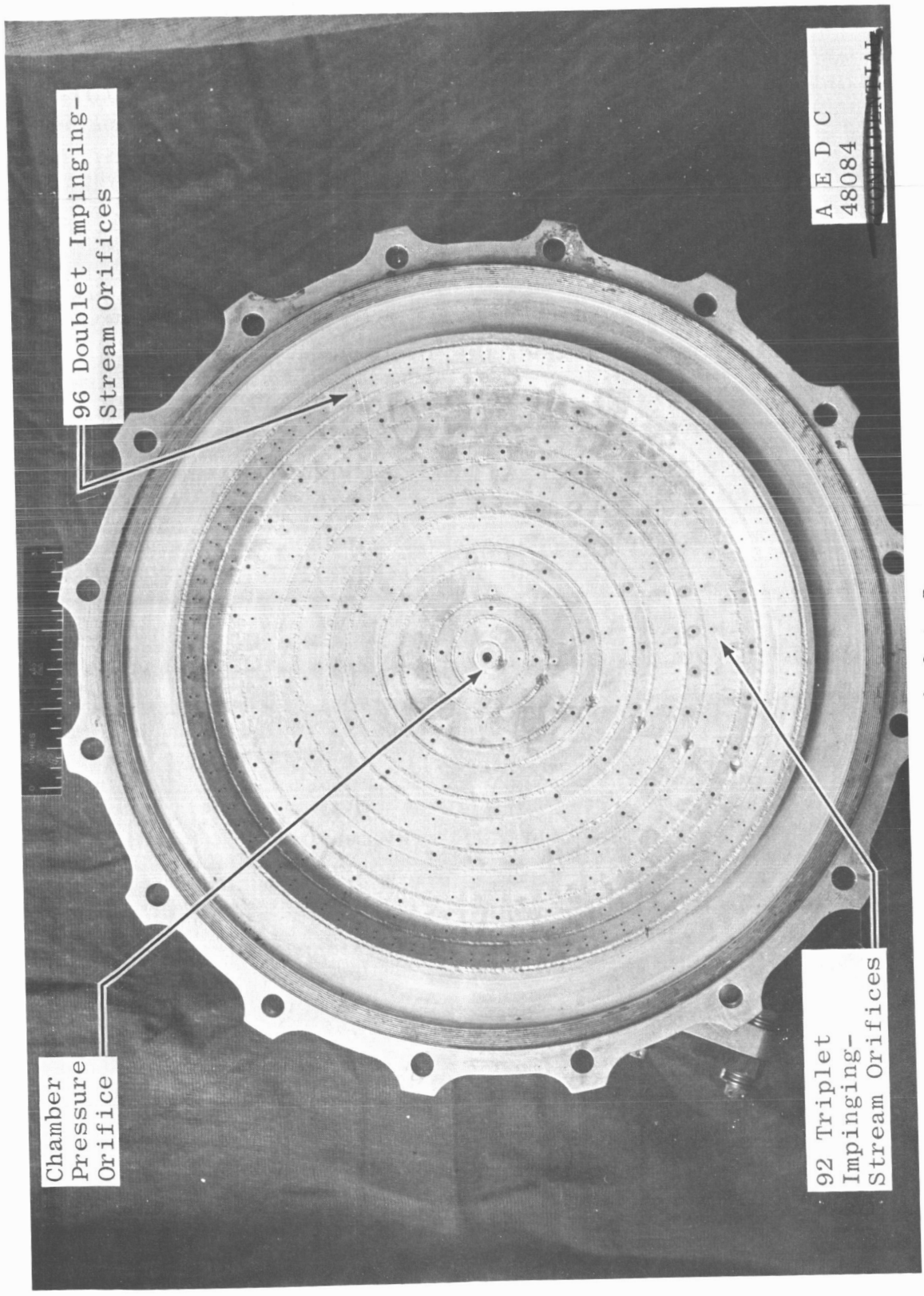

b. Series B

Fig. 4 Concluded

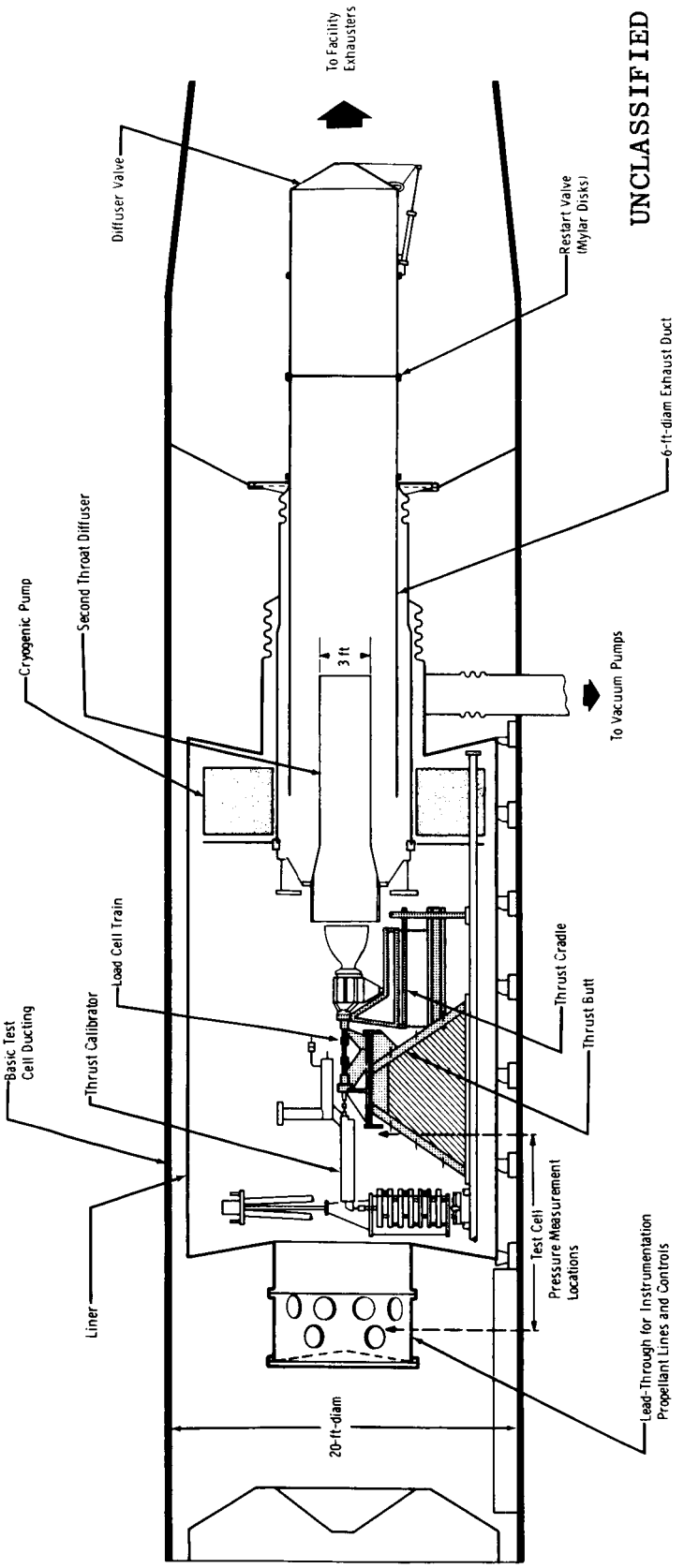

a. Test Cell Schematic

Fig. 5 Installation in Propulsion Engine Test Cell (J-2A)

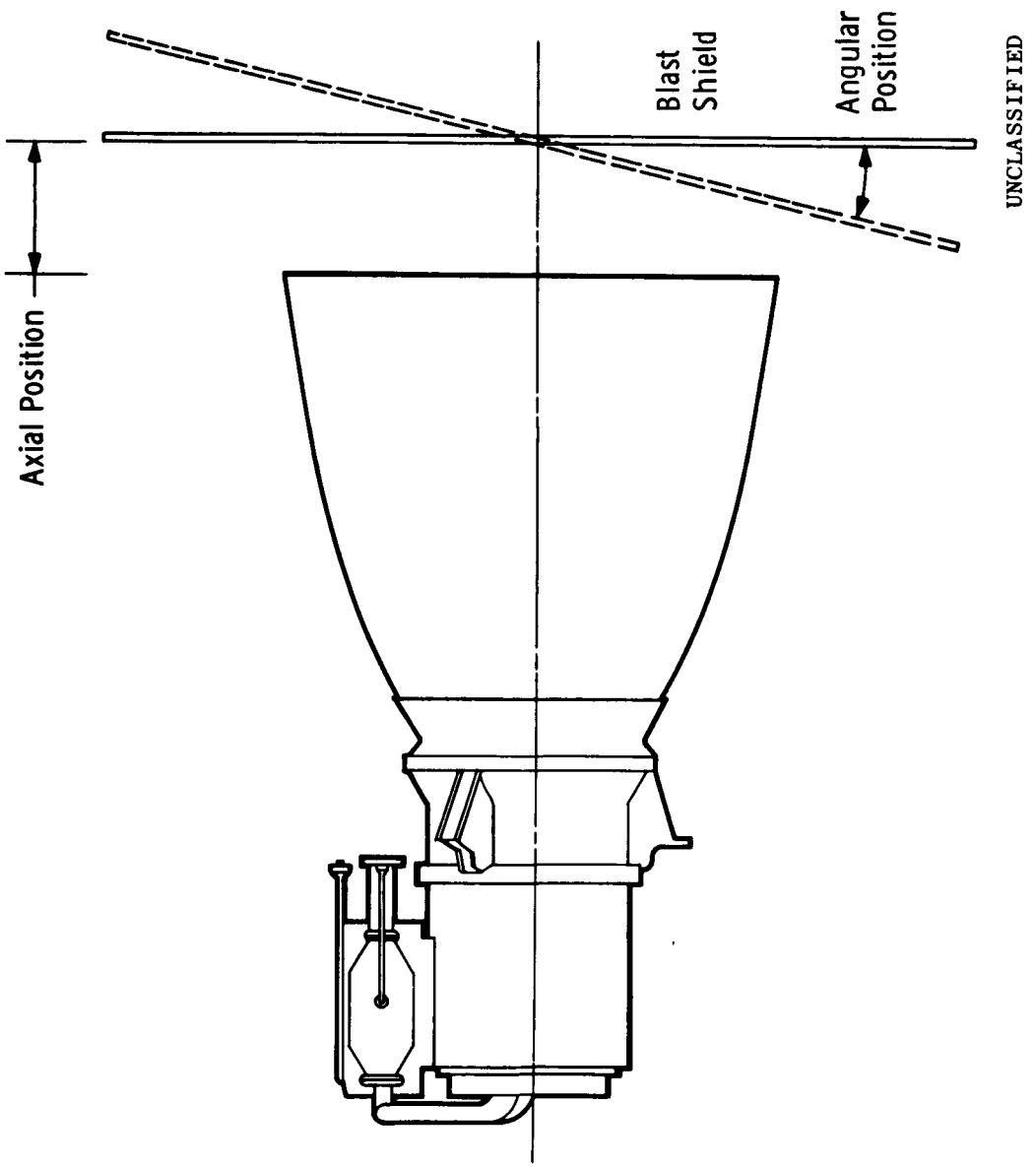

b. Blast Shield Location Schematic

Fig. 5 Concluded

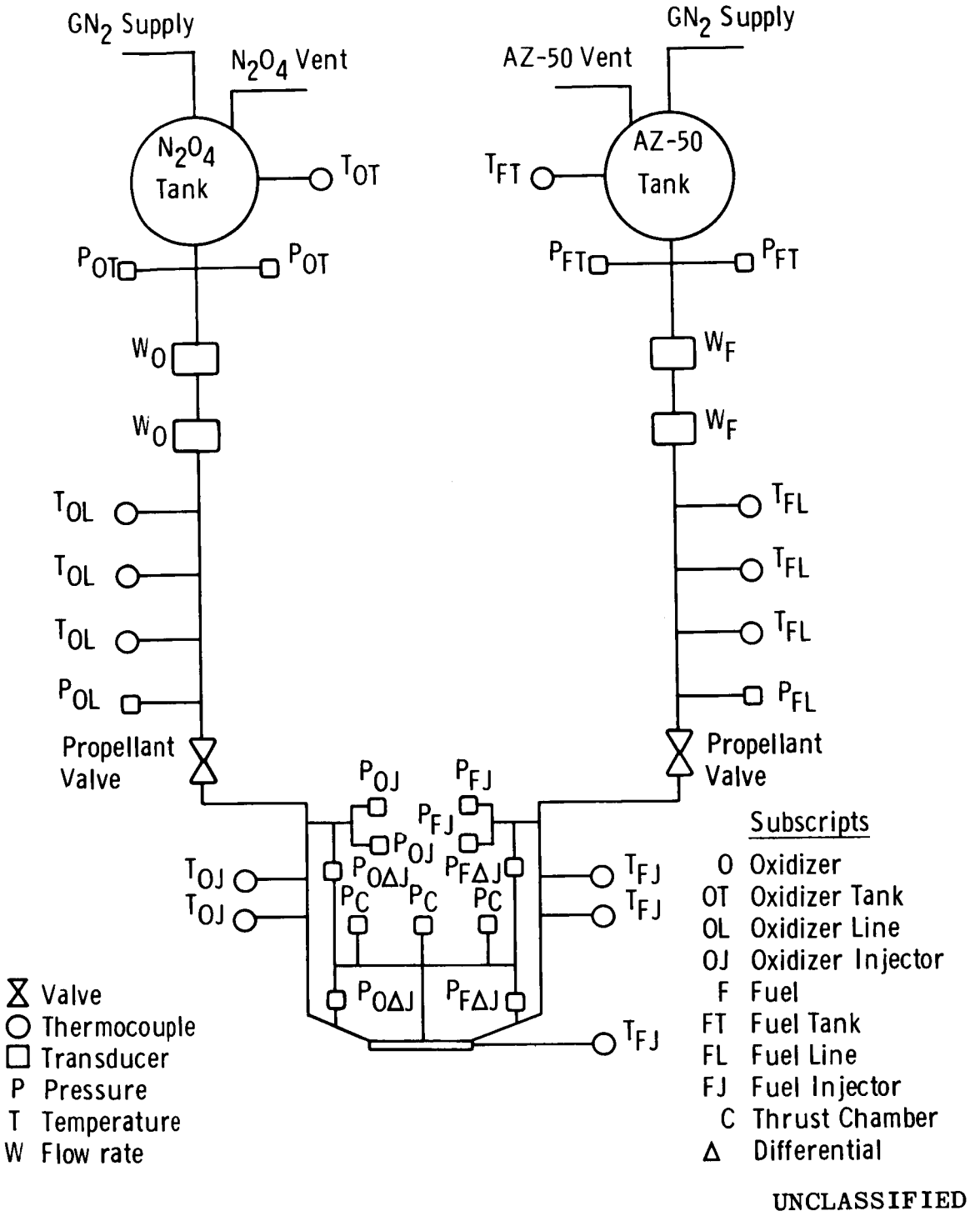

Fig. 6 Typical Propellant System Schematic

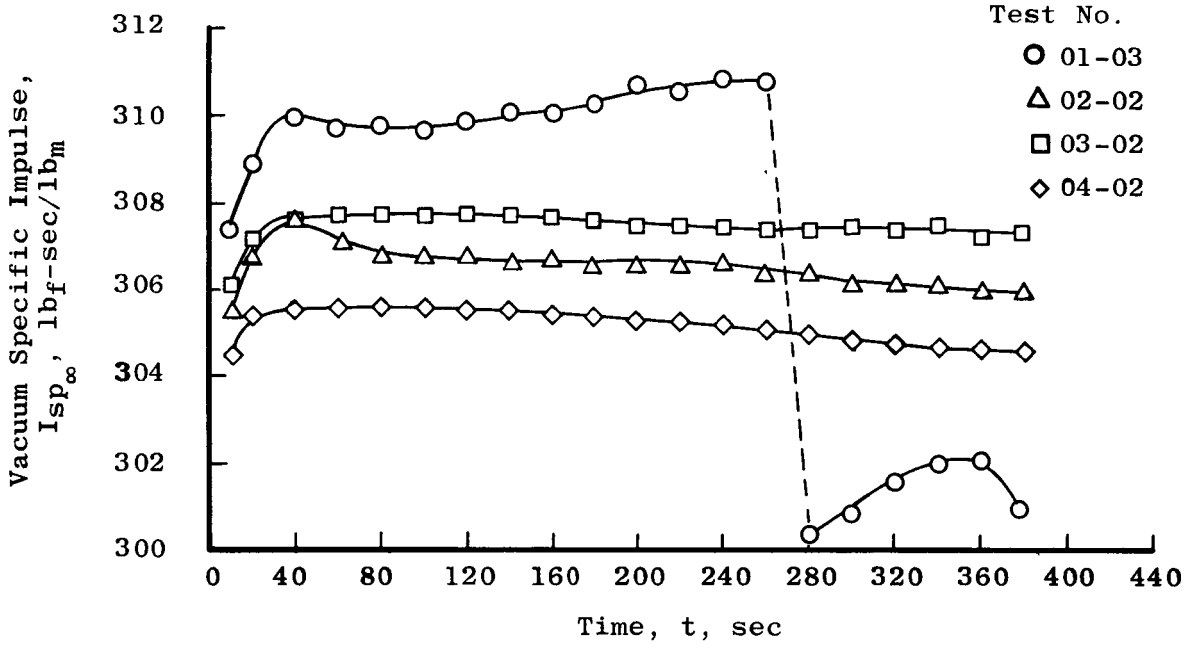

Phase I

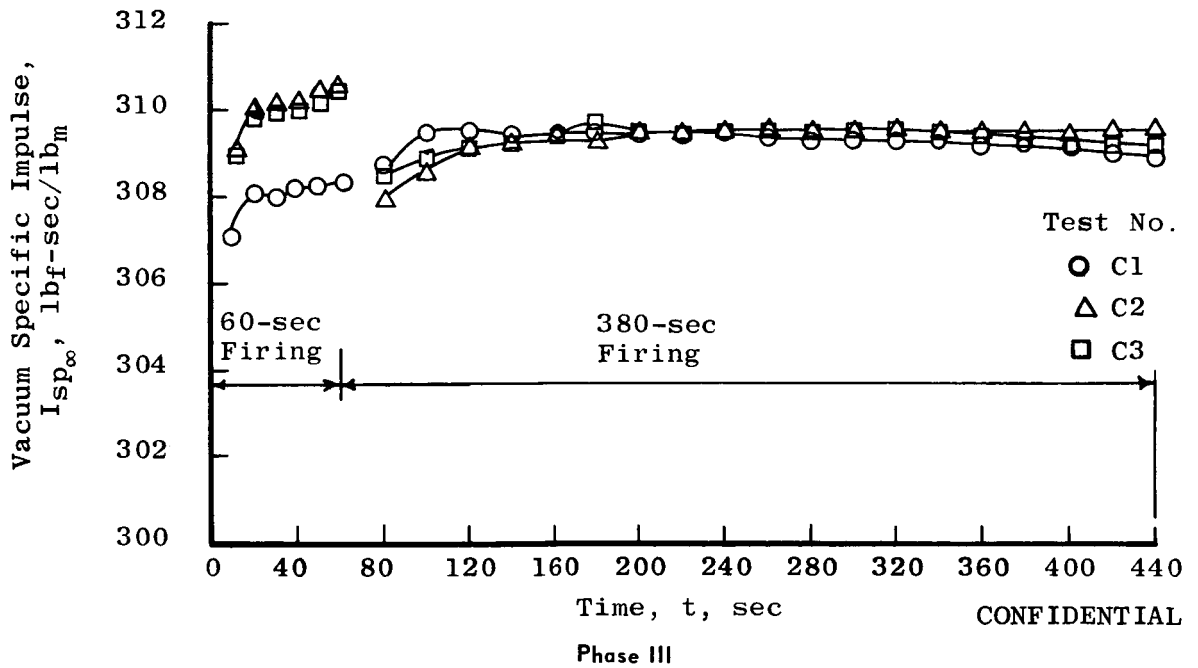

Phase III

Fig. 7 Vacuum Specific Impulse as a Function of Time

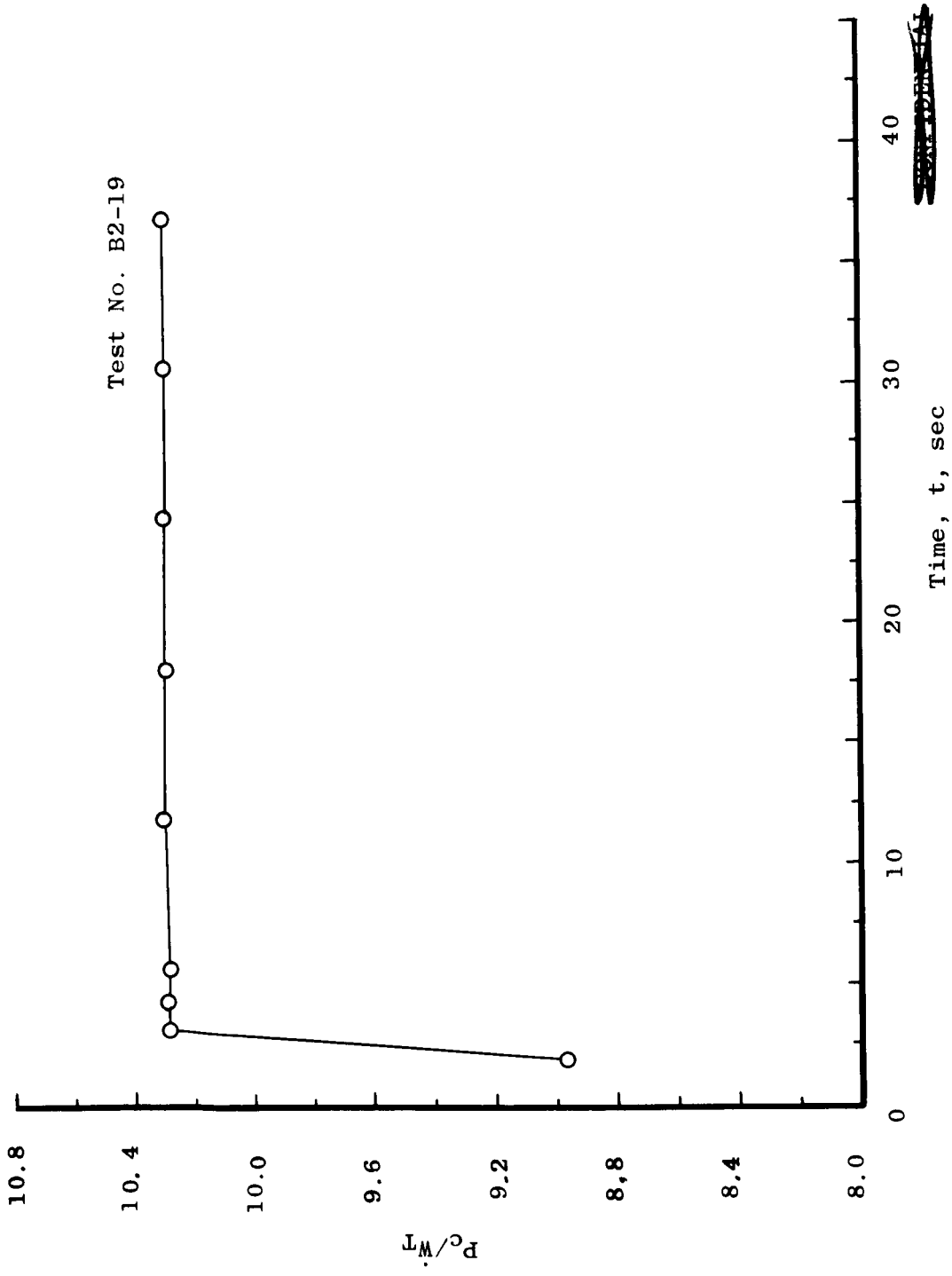

Fig. 8 Typical Variation of $P_c/\dot{W}_T$ as a Function of Time

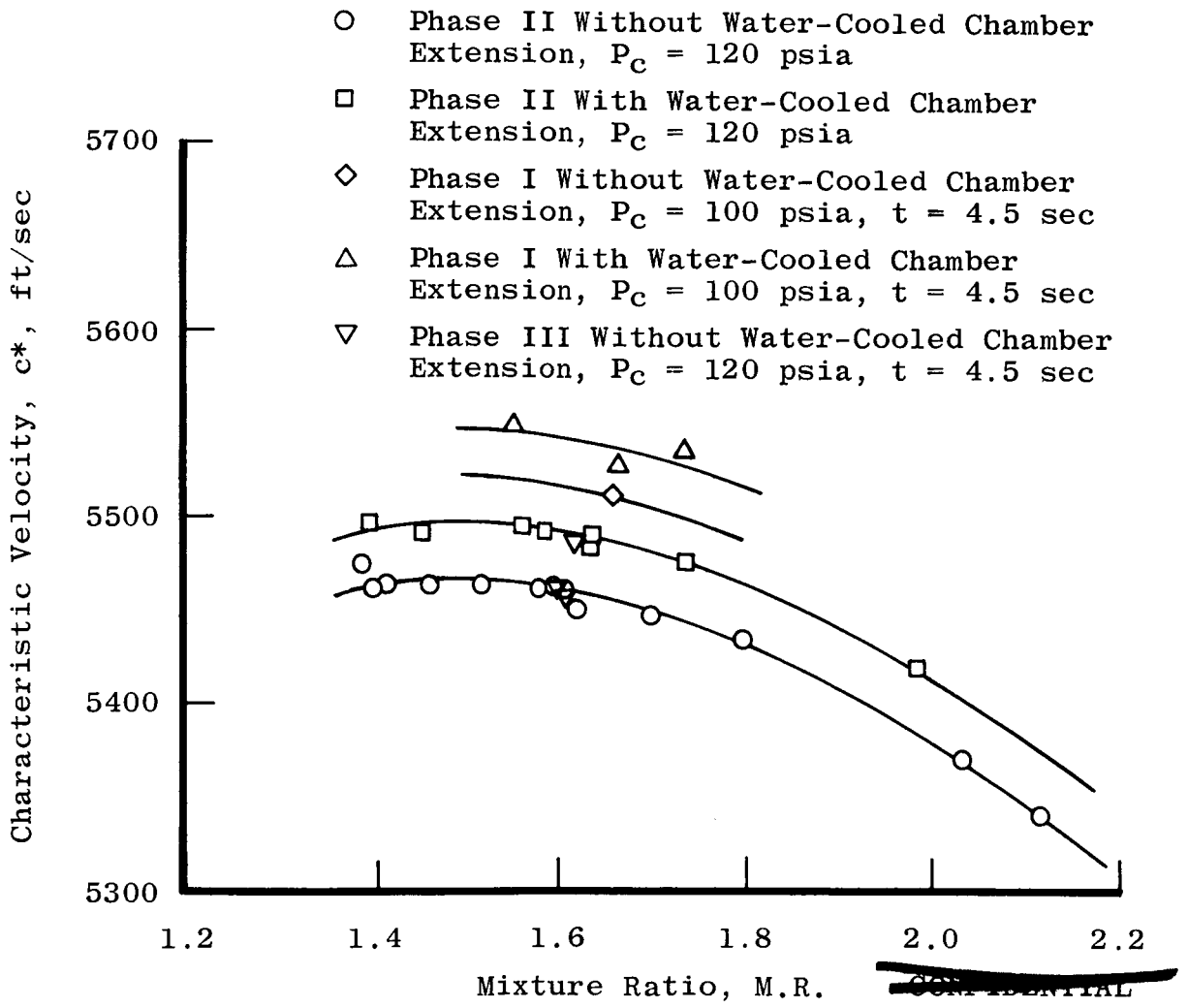

Fig. 9 Variation of Characteristic Velocity

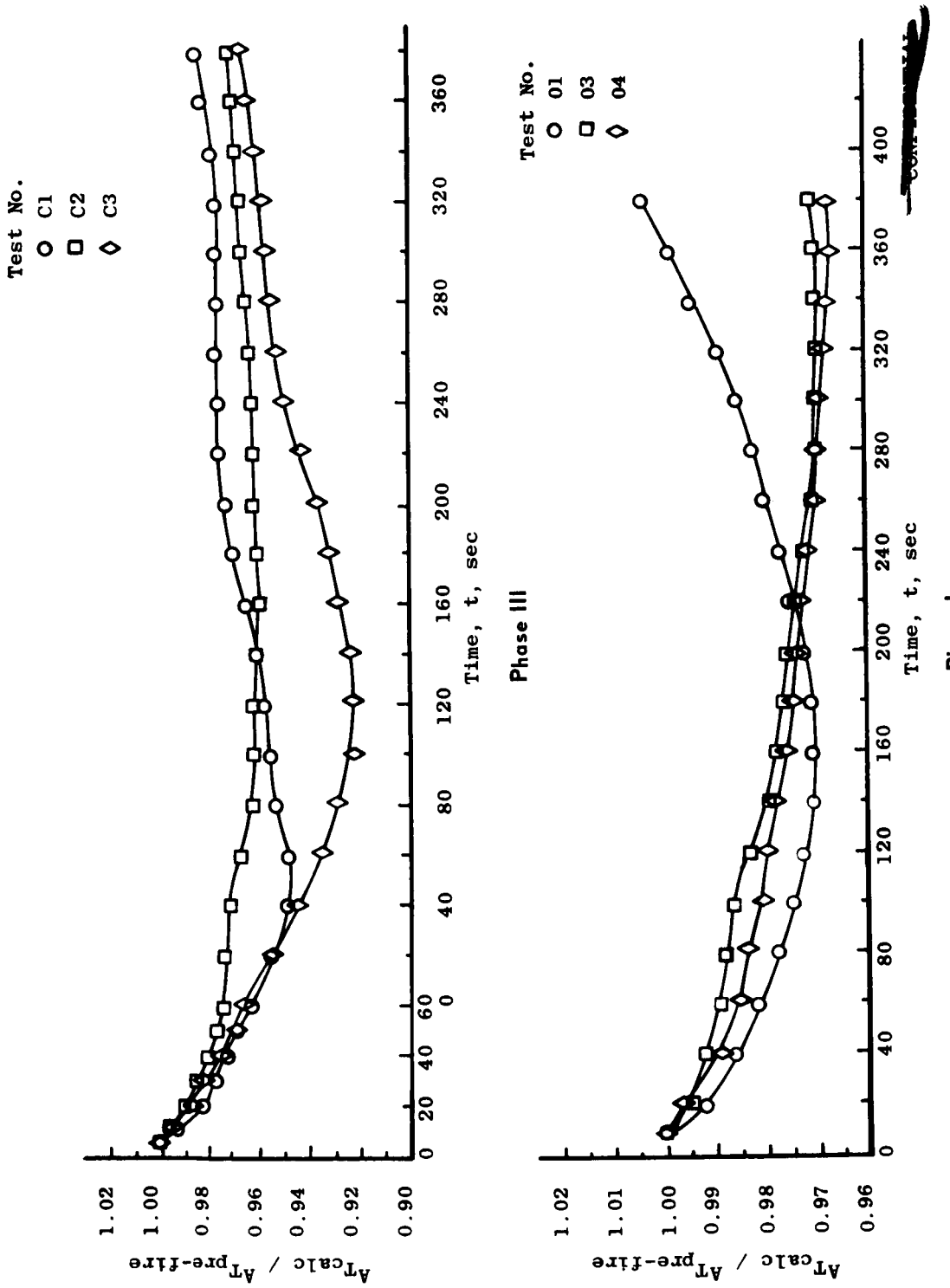

Fig. 10 Summary of Throat Area Change

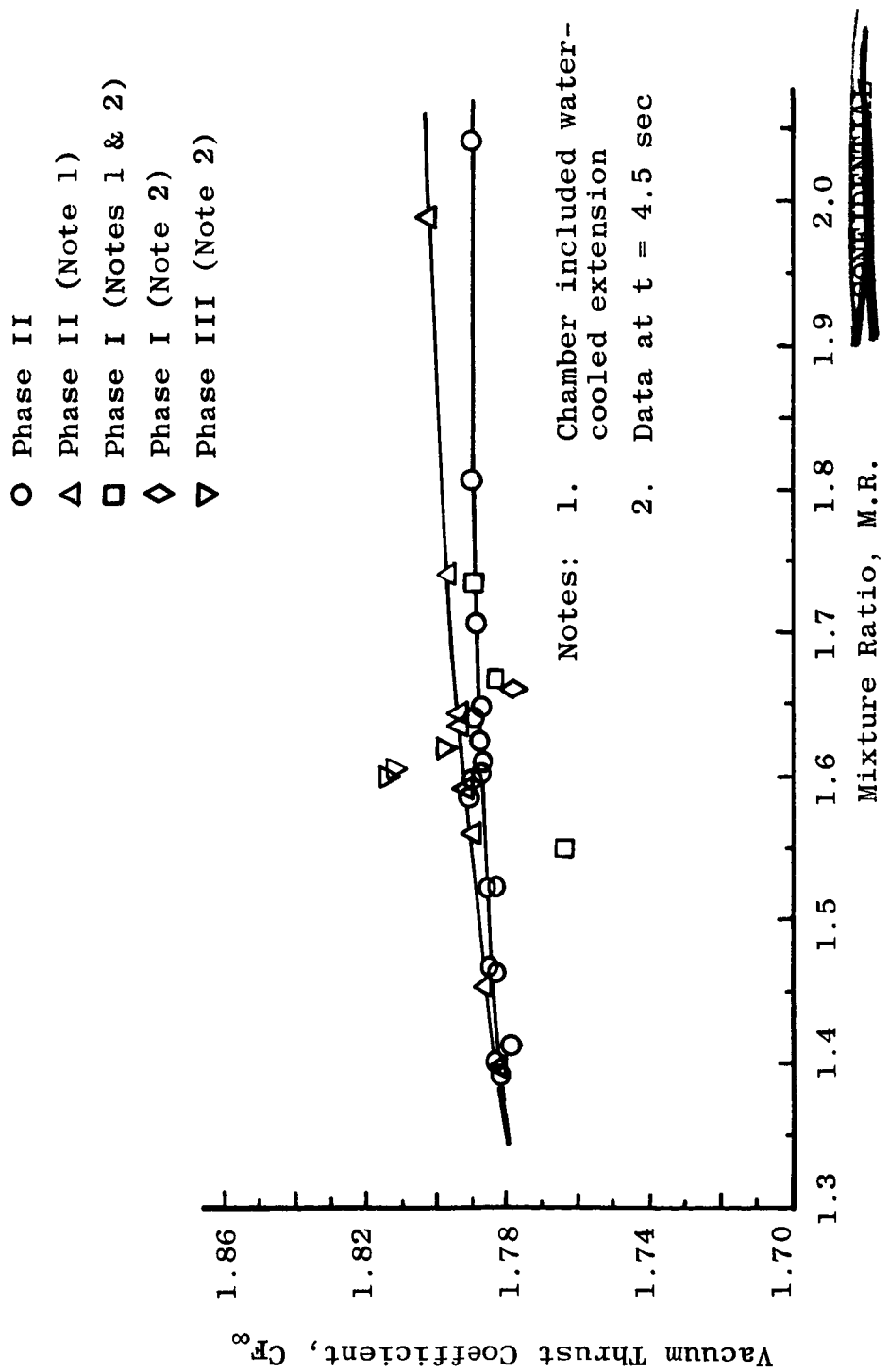

Fig. 11 Variation of Vacuum Thrust Coefficient

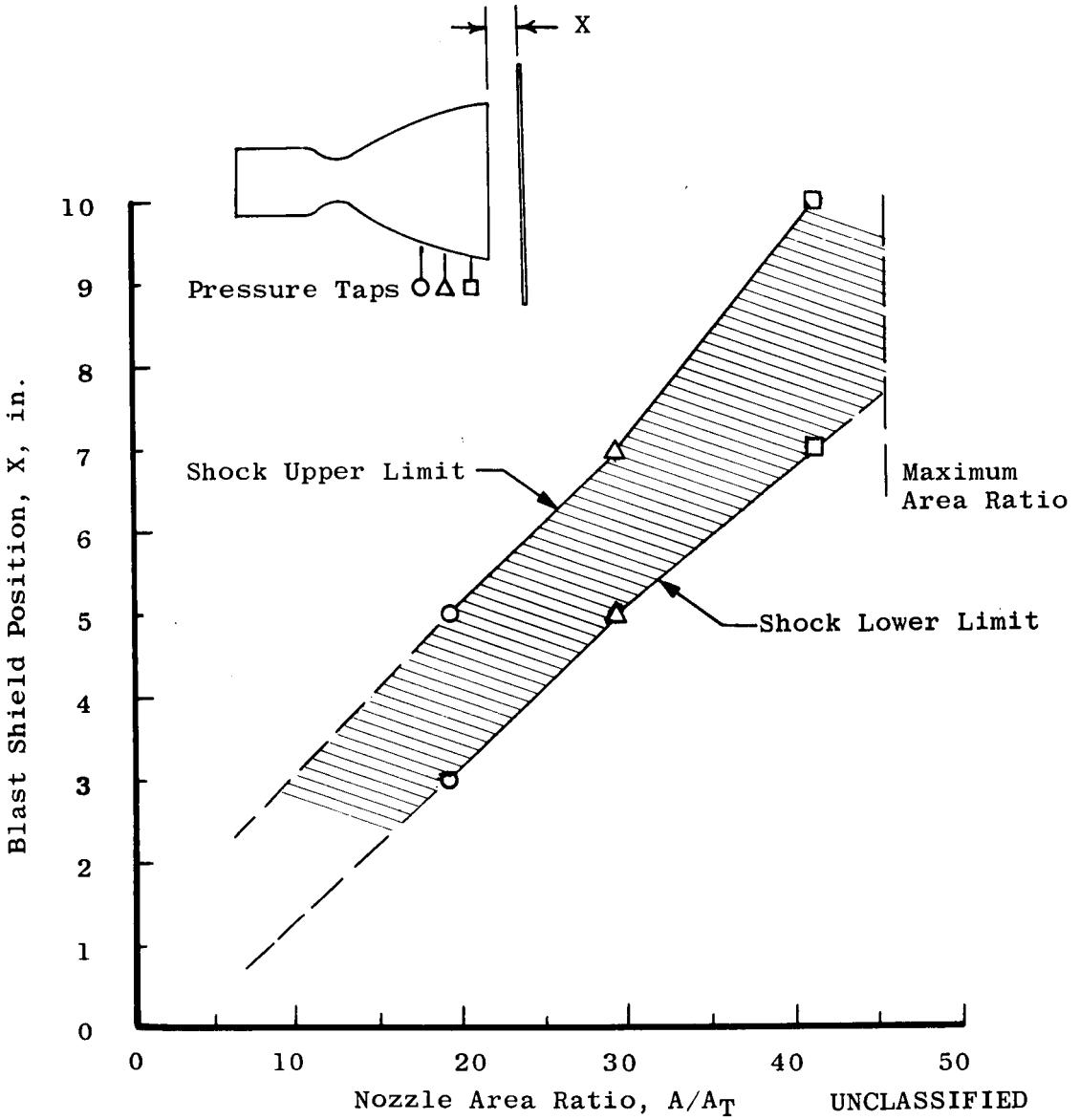

Fig. 12 Approximate Location of Shock Wave in the Engine Nozzle as a Function of Blast Shield Position

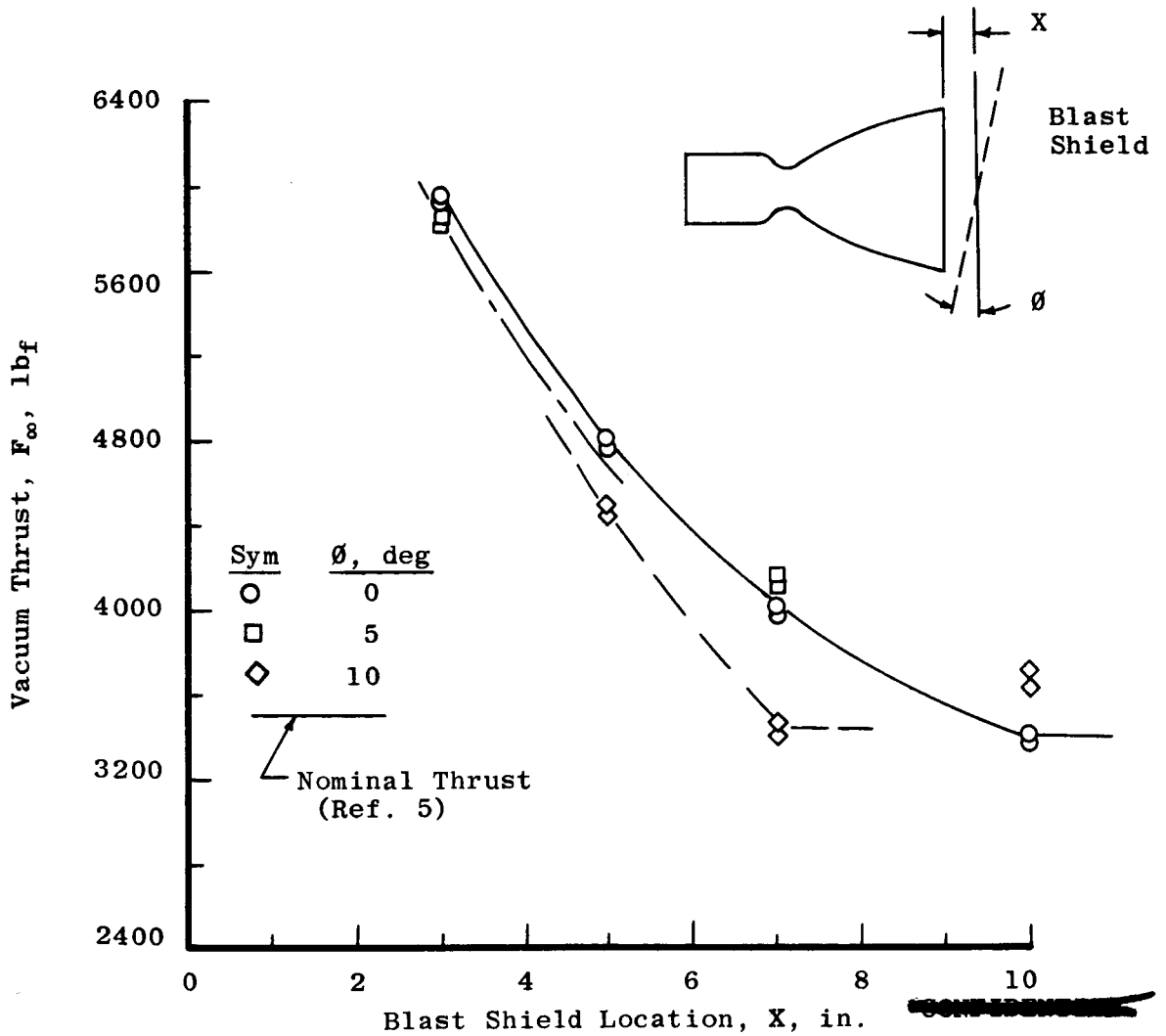

Fig. 13 Engine Vacuum Thrust as a Function of the Blast Shield Position

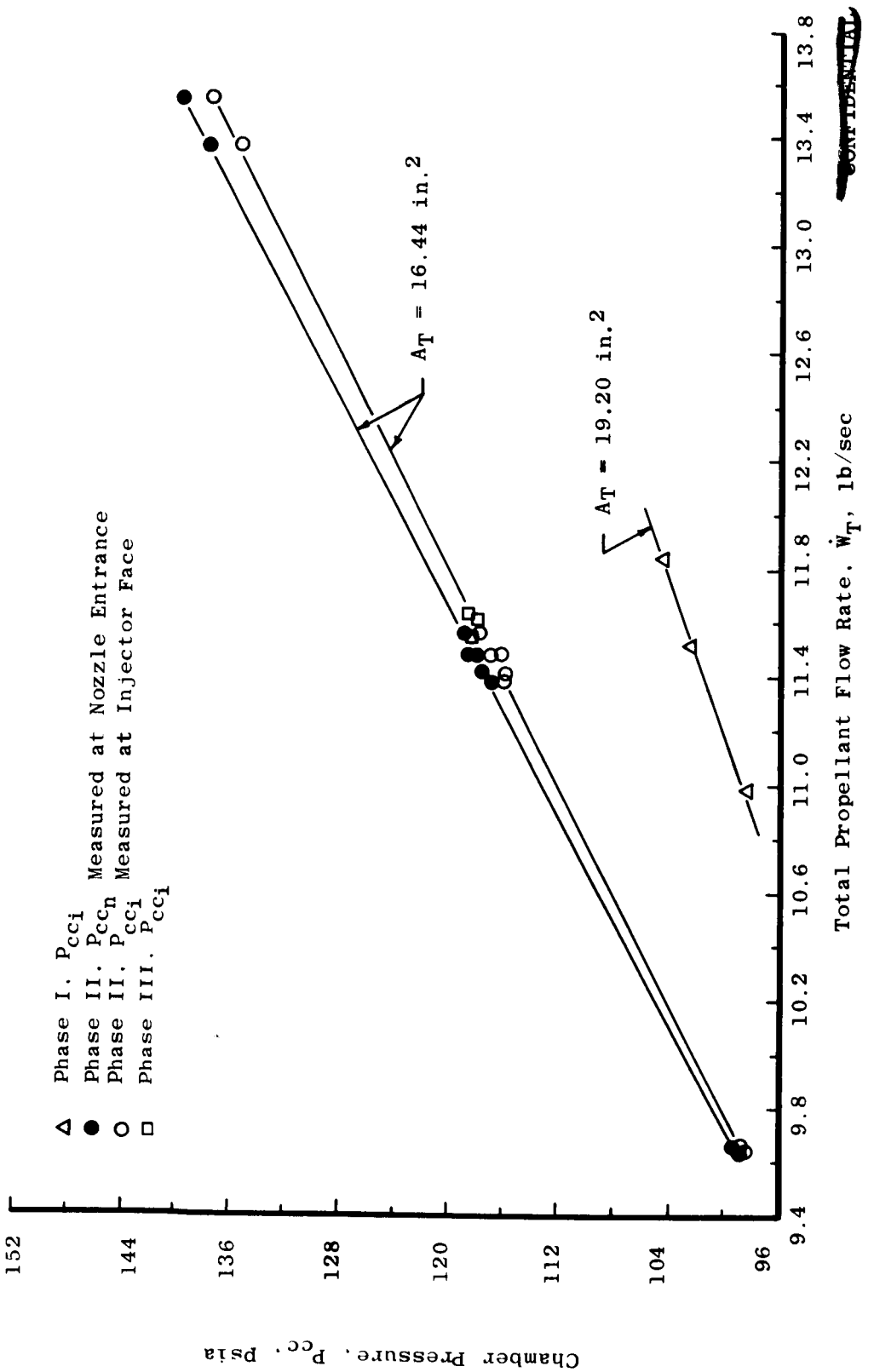

Fig. 14 Chamber Pressure versus Propellant Flow Rate at 4.5 sec

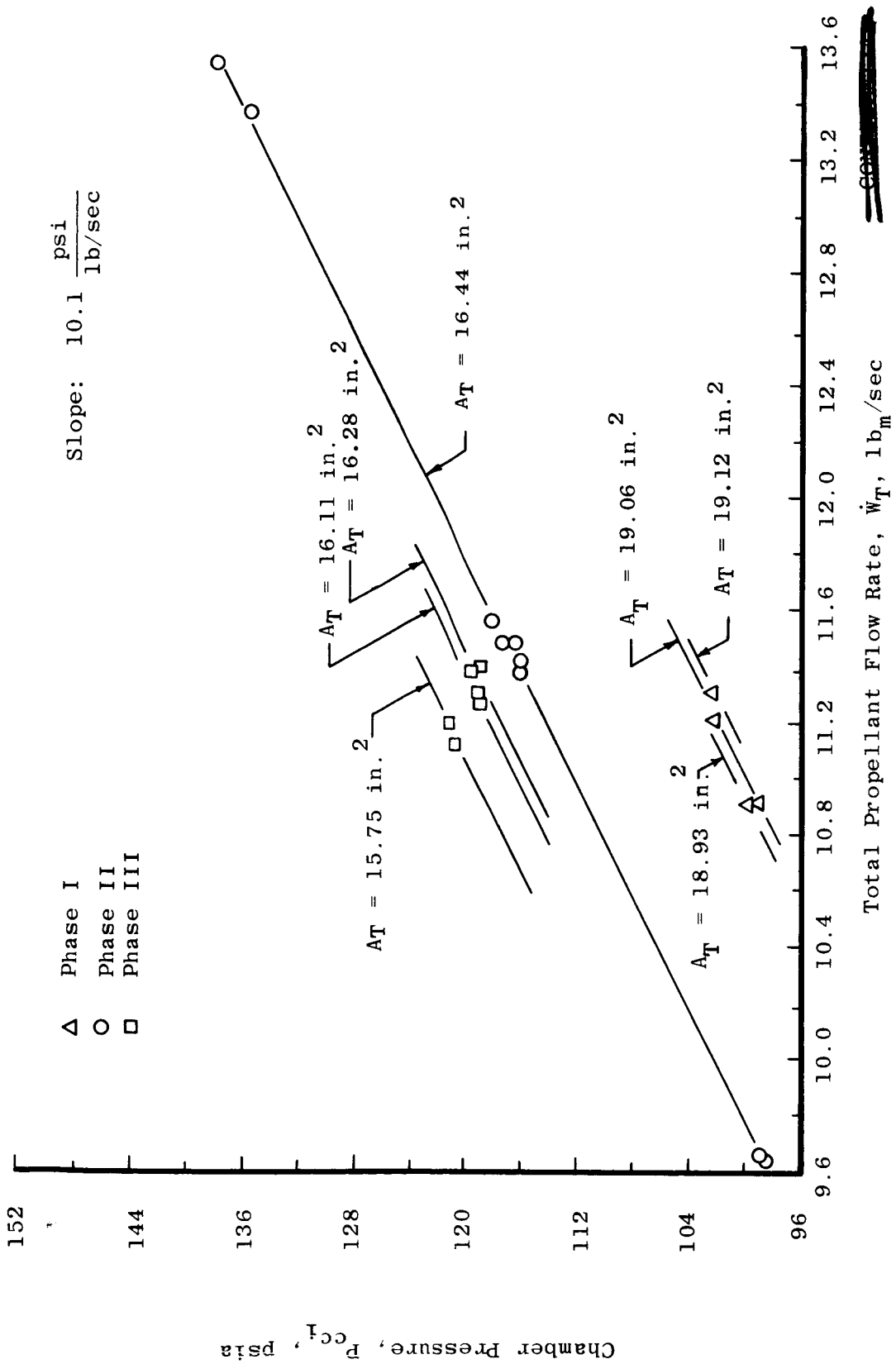

Fig. 15 Chamber Pressure versus Propellant Flow Rate at 20 sec

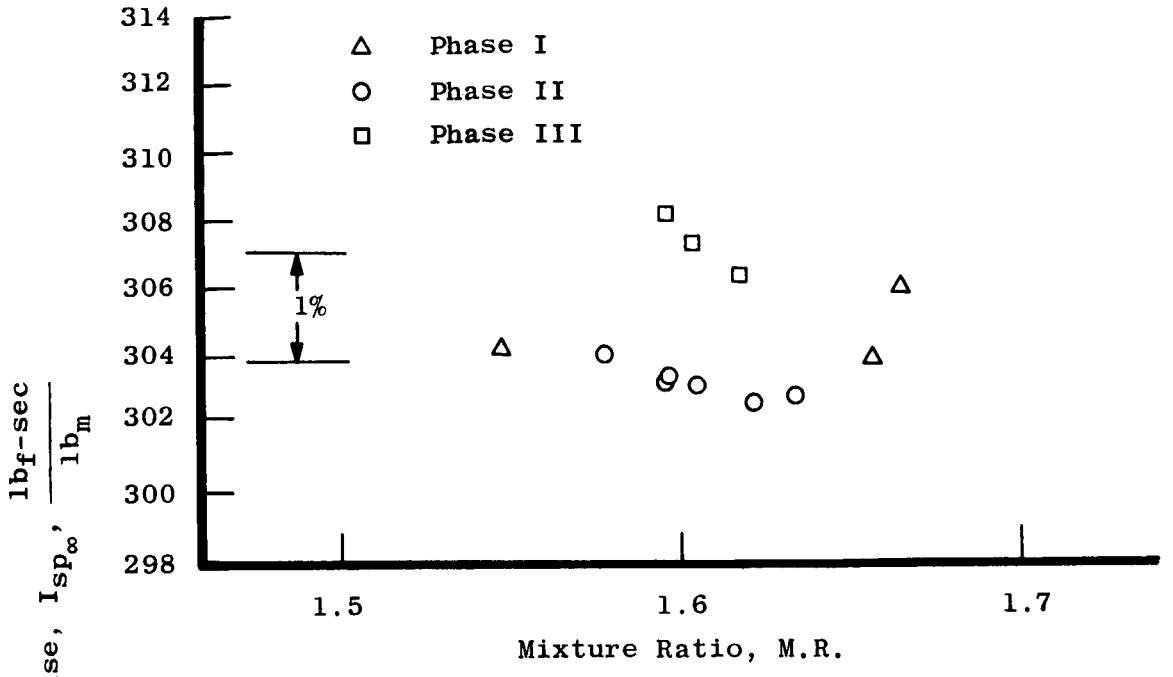

a. As Measured

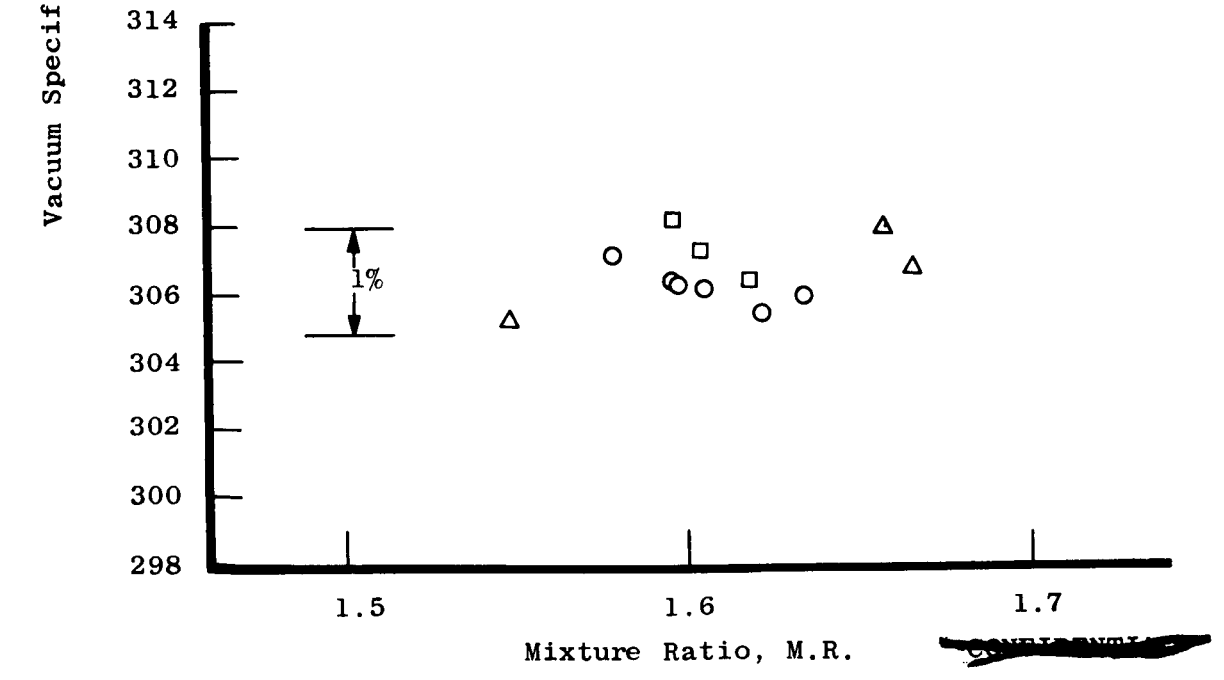

b. Adjusted

Fig. 16 Vacuum Specific Impulse at 4.5 sec

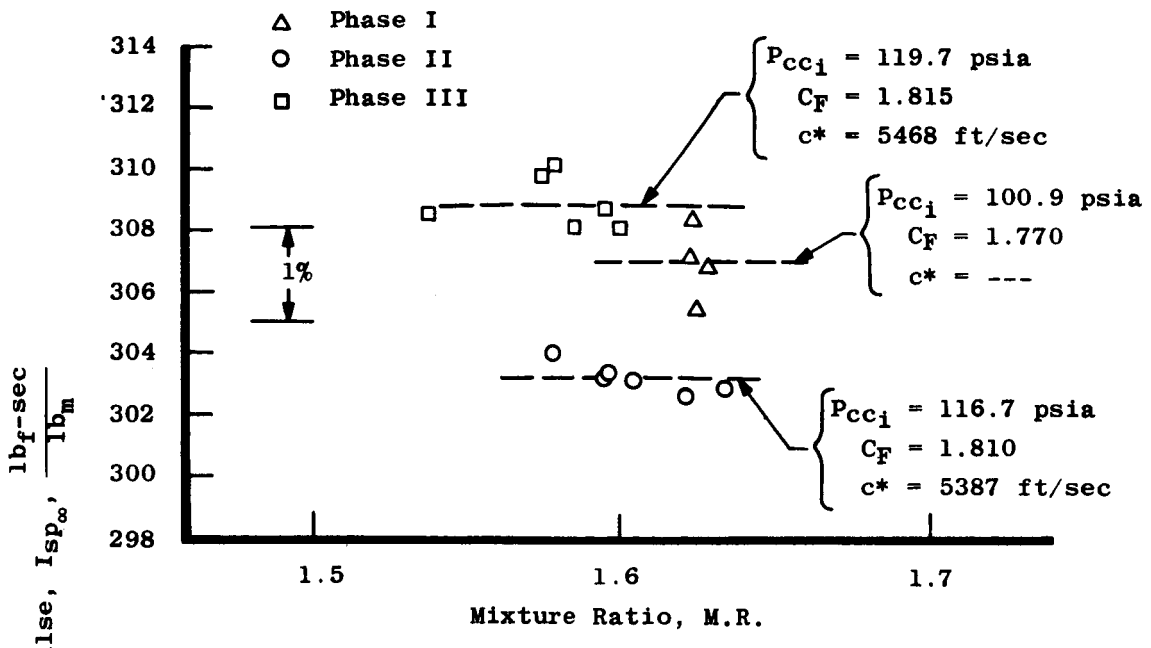

a. As Measured

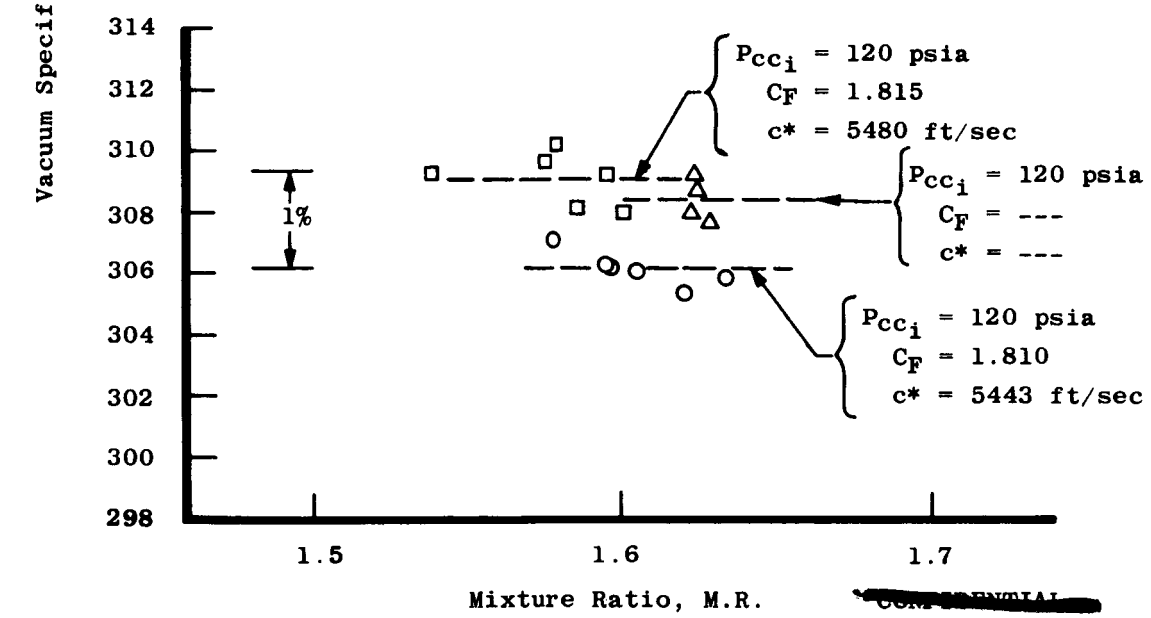

b. Adjusted

Fig. 17 Vacuum Specific Impulse at 20 sec

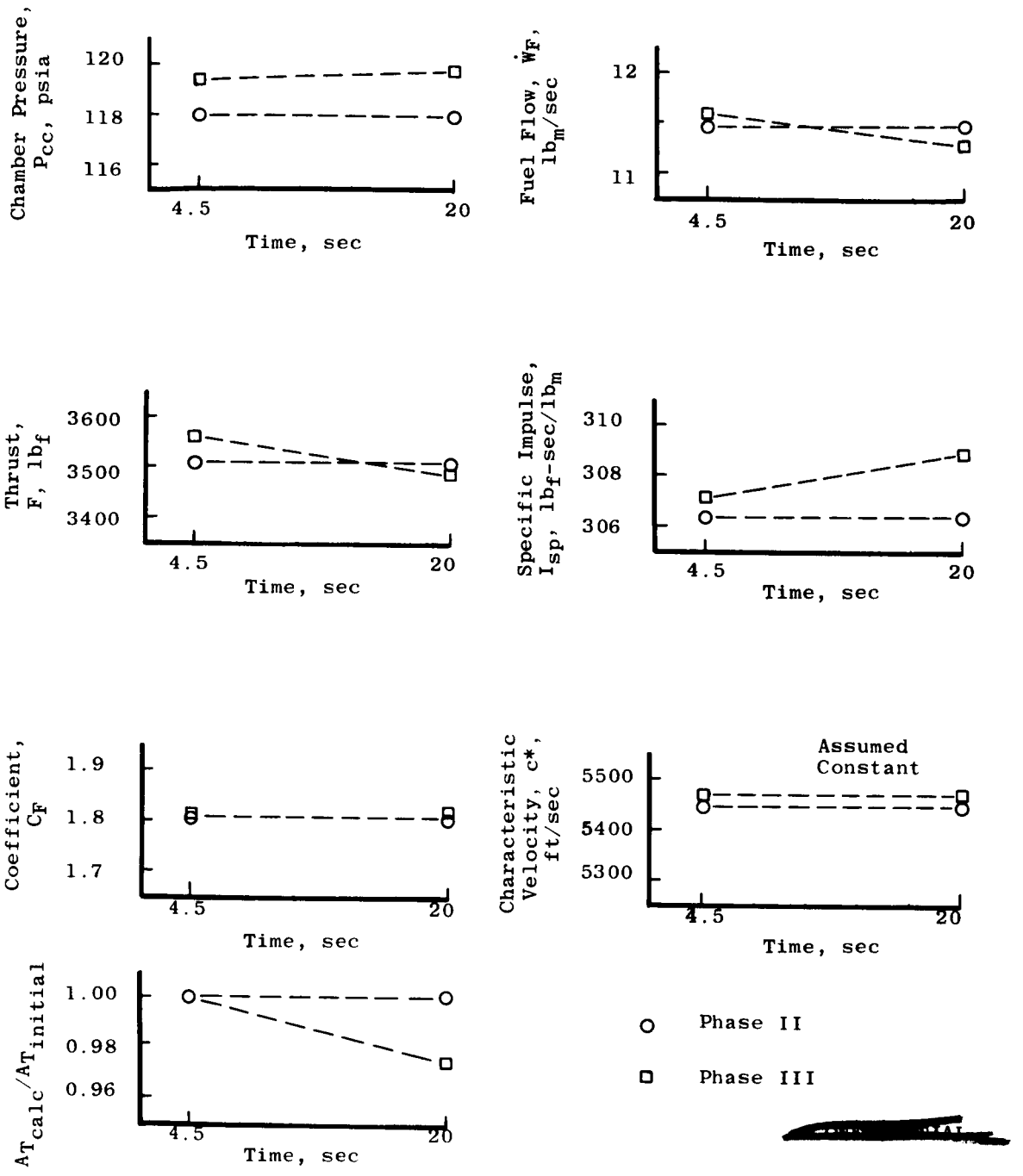

Fig. 18 Tendencies of Performance with Engine Operating Time

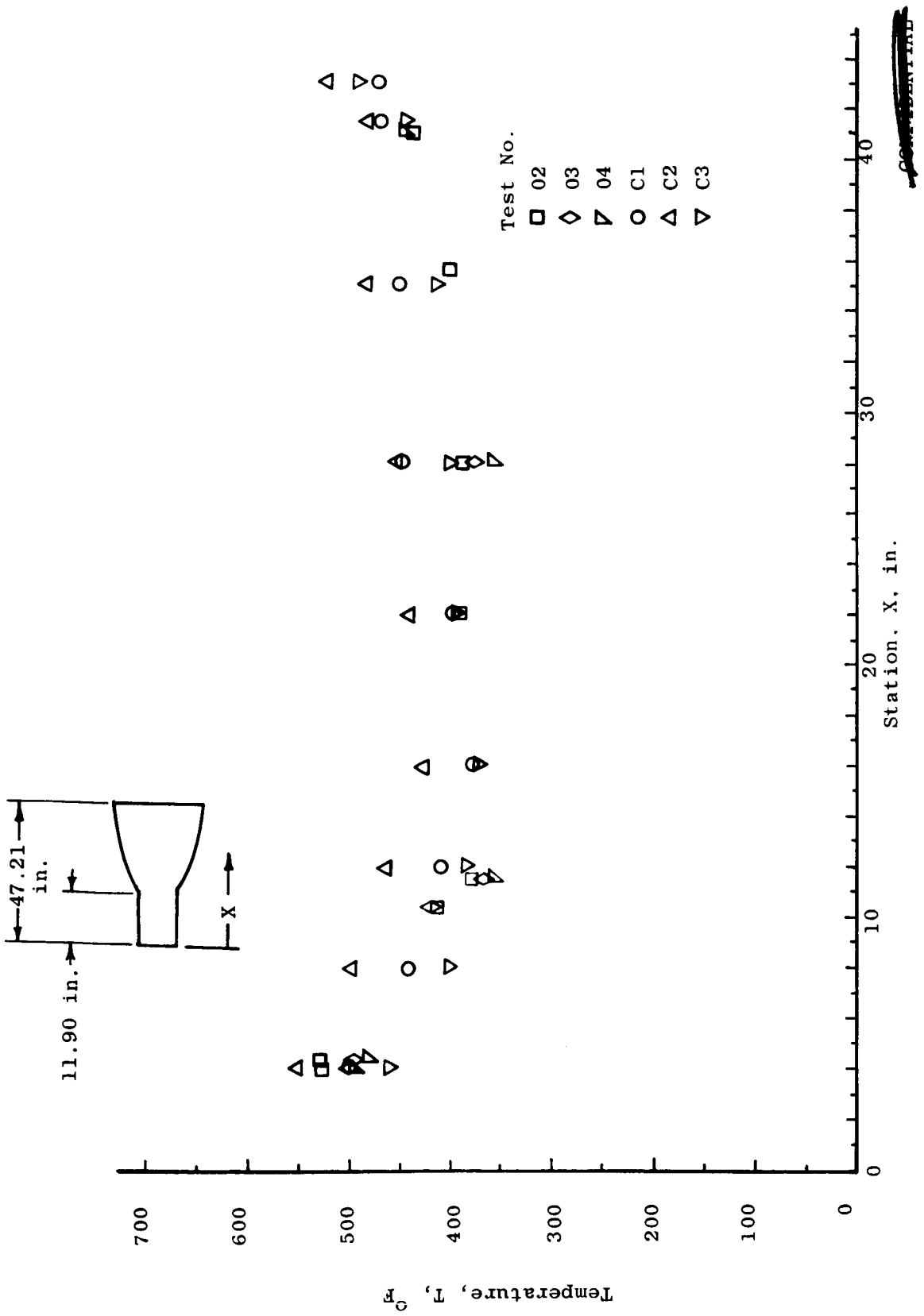

Fig. 19 Maximum External Temperatures

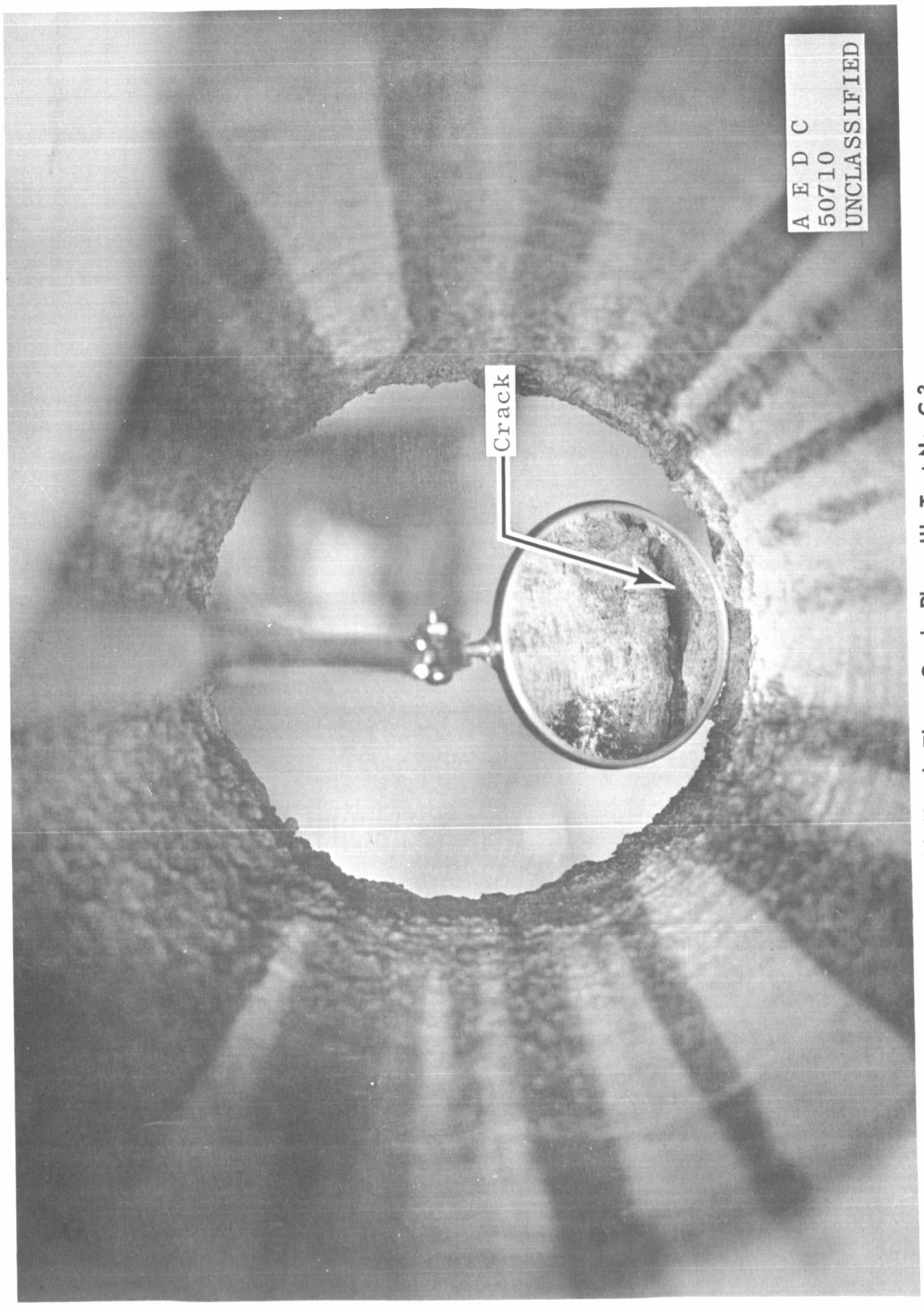

Fig. 20 Nozzle Throat Crack, Phase III, Test No. C-3

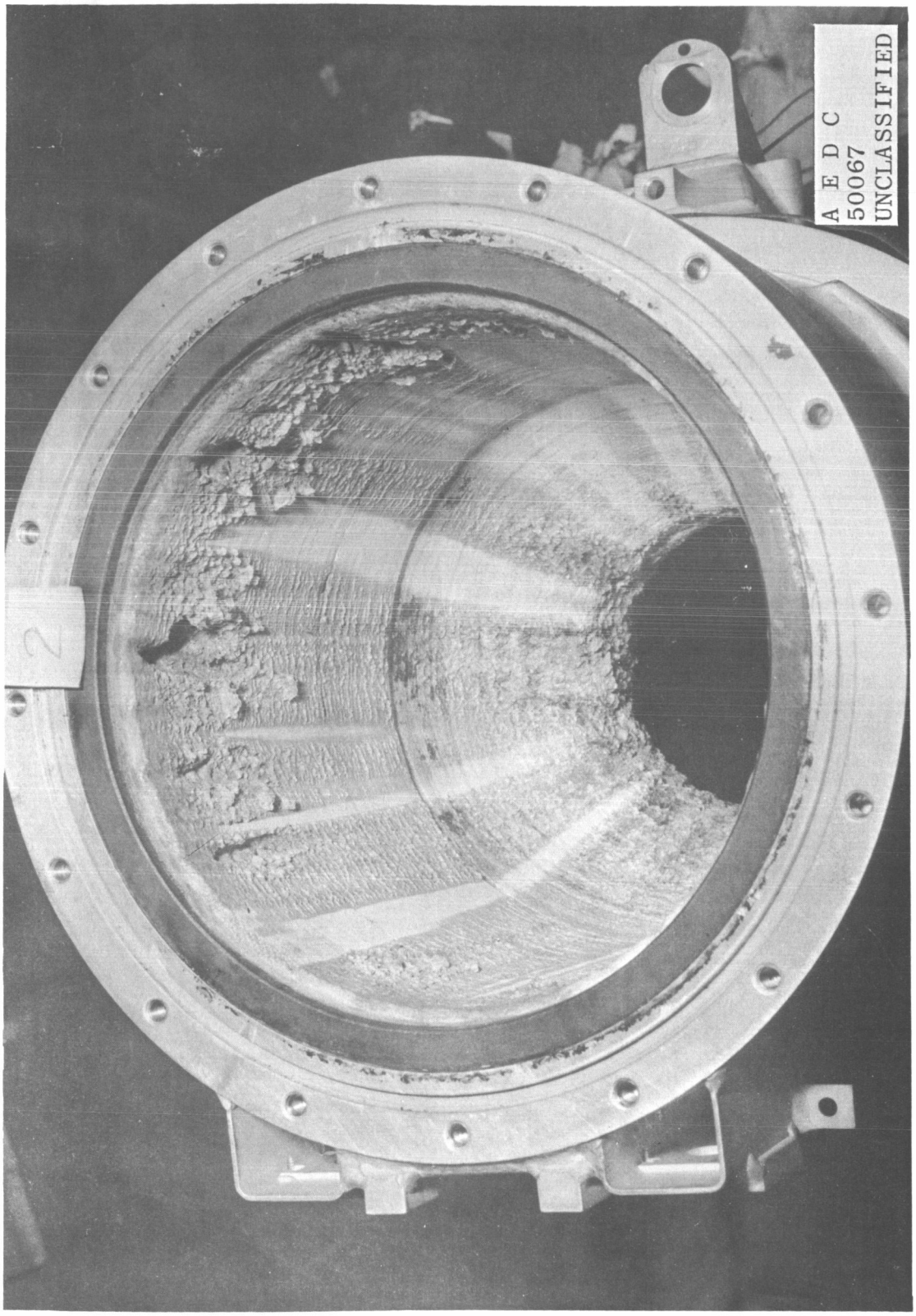

Fig. 21 Typical Post-Fire Condition of Combustion Chamber

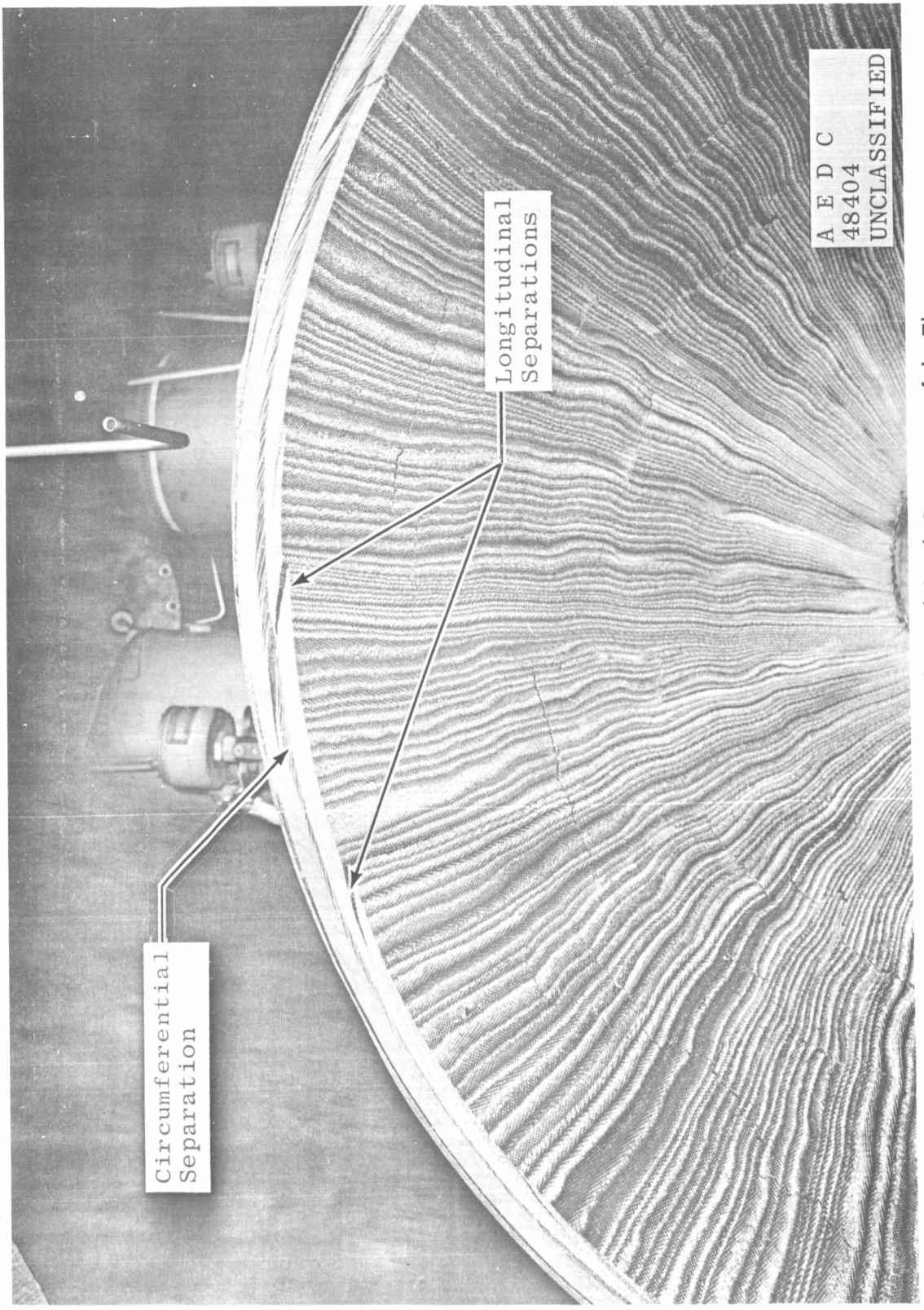

Fig. 22 Typical Post-Fire Condition of Nozzle Downstream of the Throat

TABLE I
TEST SUMMARY AND CONFIGURATIONS

Phase of Testing	Test No.	Firing No.	Thrust Chamber S/N	Area Ratio, A/A_T	Injector S/N	Firing Duration, sec	Initial Pressure Alt., ft	Final Pressure Alt., ft
I	01†	01	A-1-271-1	40:1	A3-1	5.07	80,000	87,000
		02				4.82	78,000	86,000
		03				378.2	86,000	115,000
	02†	01	H-1-300-1		A3-3	11.88	111,000	115,000
		02				380.0	80,000	126,000
		03				5.18	104,000	106,000
	03†	01	H-3-300-5			9.82	77,000	91,000
		02				379.8	111,000	127,000
		03				5.08	121,000	122,000
	04	01	H-2-300-3		B3-1	10.00	79,000	92,000
		02				379.8	117,500	129,000
		03				5.16	116,000	118,000
II	B1	1	Water-cooled	45.6:1	B3-L2	20	75,000	99,000
		2				30		105,000
		3				20		99,000
		4-10				30		105,000
	B2	13-21			B3-1	30		
	B3†	22-29				30		
III	C1	01	H-1-350-3		B3-L2	60.14	78,700	110,300
		02				379.90	78,500	120,900
		03				4.90	112,800	114,000
	C2	01	H-2-350-3			59.90	76,800	107,600
		02				380.10	76,800	115,800
		03				5.07	78,300	85,500
	C3	01	H-3-350-3			59.20	76,200	109,000
		02				379.70	75,200	116,200
		03				5.09	86,000	81,600
IV	D4	1-18	H-1-430-1			0.650	88,000	66,000

† These configurations included a 4.125-in., water-cooled combustion chamber extension.

TABLE II
DATA SUMMARY AT 20 SEC

Test	M. R.	P_{cc}, psia	$\dot{W}_T$, lb_m	F_∞, lb_f	$I_{sp\infty}$, lb_f-sec/lb_m	C_F	A/A_T†	Injector Type
01-03	1.624	99.98	10.91	3370	308.9	1.771	40	A
02-02	1.629	102.41	11.21	3440	306.8	1.760	40	A
03-02	1.623	102.36	11.31	3474	307.2	1.778	40	A
04-02	1.625	98.90	10.92	3335	305.4	1.772	40	B
B1-1	1.516	118.3	11.46	3468	302.8	1.784	45.6	↓
B1-2	1.518	99.78	9.66	2907	300.8	1.781	↓	↓
B1-3	1.464	140.18	13.55	4114	304.0	1.784	↓	↓
B1-4	1.388	119.73	11.58	3504	302.8	1.780	↓	↓
B1-5	1.634	118.25	11.48	3475	302.8	1.788	↓	↓
B1-6	2.113	117.90	11.69	3476	297.3	1.793	↓	↓
B1-7	1.643	98.52	9.64	2894	300.3	1.787	↓	↓
B1-8	1.621	117.17	11.38	3442	302.6	1.787	↓	↓
B1-9	1.593	138.21	13.36	4064	304.2	1.789	↓	↓
B1-10	1.411	118.63	11.49	3465	301.7	1.777	↓	↓
B2-13	1.578	119.34	11.56	3514	304.0	1.791	↓	↓
B2-14	1.460	114.91	11.13	3366	302.6	1.782	↓	↓
B2-15	1.700	118.83	11.54	3493	302.6	1.788	↓	↓
B2-16	2.035	119.17	11.75	3507	298.6	1.790	↓	↓
B2-17	1.605	118.50	11.48	3479	303.1	1.786	↓	↓
B2-18	1.399	118.17	11.45	3462	302.3	1.782	↓	↓
B2-19	1.597	117.81	11.41	3461	303.3	1.787	↓	↓
B2-20	1.596	117.84	11.42	3461	303.2	1.787	↓	↓
B2-21	1.799	119.03	11.59	3503	302.3	1.790	↓	↓
B3-22	1.736	116.38	11.25	3435	305.5	1.796	↓	↓
B3-23	1.451	118.03	11.37	3461	304.4	1.784	↓	↓
B3-24	1.632	117.87	11.37	3475	305.6	1.794	↓	↓
B3-25	1.982	119.39	11.65	3537	303.5	1.802	↓	↓
B3-26	1.583	119.31	11.49	3514	305.7	1.791	↓	↓
B3-27	1.391	118.44	11.40	3466	304.1	1.780	↓	↓
B3-28	1.559	117.66	11.33	3461	305.5	1.789	↓	↓
C1-01	1.586	119.10	11.30	3481	308.1	1.807	↓	↓
C1-02	1.596	120.77	11.12	3434	308.7	1.806	↓	↓
C2-01	1.579	118.81	11.40	3537	310.2	1.824	↓	↓
C2-02	1.601	118.98	11.27	3473	308.1	1.817	↓	↓
C3-01	1.575	119.53	11.38	3526	309.8	1.821	↓	↓
C3-02	1.538	121.15	11.19	3454	308.5	1.818	↓	↓

† Approximate Pre-Fire Area Ratio

TABLE III
NOZZLE PRESSURE MEASUREMENTS

Phase IV Firing No.	Blast Shield Position		Pressure Tap Location								
			A/A_T = 19.2			A/A_T = 29.2			A/A_T = 41.4		
	Axial, in.	Angle, deg	0 deg	180 deg	270 deg	0 deg	180 deg	270 deg	0 deg	180 deg	270 deg
1	5	0	1.05	0.95	0.95	2.9	2.9	3.2	4.5	4.1	5.0
2	5	0	1.00	0.95	0.90	3.0	3.2	2.9	5.3	4.5	4.6
3	5	10	1.25	0.90	0.95	2.3	2.1	2.3	4.5	-	2.9
4	5	10	1.40	0.95	0.80	2.4	2.0	2.3	4.5	-	2.9
5	7	0	1.00	0.90	0.80	0.35	0.55	0.80	5.3	-	4.2
6	7	0	0.95	0.85	0.85	0.45	0.60	0.55	5.0	-	4.1
7	7	5	0.95	0.90	0.80	0.35	0.60	0.60	4.5	-	5.7
8	7	5	1.20	0.90	0.85	0.45	0.55	0.55	4.8	-	5.7
9	7	10	0.95	0.90	0.75	0.45	0.50	0.55	0.40	-	0.30
10	7	10	1.00	0.90	0.80	0.30	0.60	0.60	0.50	-	0.40
11	3	0	3.9	3.5	3.9	4.5	5.5	4.7	6.0	-	5.9
12	3	0	3.5	4.2	4.2	6.0	4.2	4.5	6.0	-	6.0
13	3	5	2.6	3.8	4.0	5.0	4.0	4.3	5.7	-	5.3
14	3	5	2.5	3.7	4.0	5.0	3.9	4.5	5.4	-	5.2
15	10	0	1.00	0.96	0.95	0.74	0.75	0.60	0.40	0.47	0.39
16	10	0	1.00	0.94	0.95	0.72	0.73	0.60	0.40	0.45	0.40
17	10	10	1.00	0.95	0.95	-	-	0.63	0.45	0.45	0.40
18	10	10	1.00	0.95	0.96	0.65	-	0.63	0.42	0.45	0.40

Notes:
1. Mean values obtained T = 0.650 sec
2. Pressure tap locations are looking upstream
3. Pressure values recorded are in psia

TABLE IV
PERFORMANCE DATA ADJUSTMENT AT 4.5 SEC

Item	Firing No.	M. R.	$\dot{W}_T$, $\frac{lb_m}{sec}$	P_{cc_i}, psia	P_{cc_n}, psia	F_∞, lb_f	I_{sp_∞}, $\frac{lb_f\text{-sec}}{lb_m}$	C_{F_i}	C_{F_N}	c^*_i, $\frac{ft}{sec}$	c^*_N, $\frac{ft}{sec}$	$F_{\infty_{adj}}$, lb_f	$I_{sp_{adj}}$, $\frac{lb_f}{lb_m/sec}$	$C_{F_{adj}}$,	c^*_{adj}, $\frac{ft}{sec}$	$P_{cc_i}A'$, $\frac{lb}{in.^2}$	F_∞, lb_f	C_F	$\frac{A^*_{calc}}{A^*_{initial}}$
								Phase I											
1	02-01	1.666	11.82	105.5	---	3617	306.0	1.783	---	5524	---	---	306.7	---	---				1.00
2	03-01	1.548	11.52	103.4	---	3505	304.2	1.764	---	5547	---	---	305.2	---	---				
3	04-01	1.657	10.99	98.4	---	3339	303.9	1.774	---	5510	---	---	307.9	---	---				
	avg	1.624	11.44	102.4	---	3487	304.7	1.774	---	5527	---	---	306.6	---	---				
								Phase II											
1	B1-5	1.634	11.48	117.3	118.3	3475	302.8	1.802	1.788	5409	5449	3555	305.9	1.802	5467	118.6	3513	1.802	1.00
2	B1-8	1.621	11.38	116.2	117.2	3442	302.6	1.802	1.787	5400	5448	3555	305.4	1.802	5457	117.4	3479	1.802	
3	B2-13	1.578	11.56	118.1	119.3	3514	304.0	1.810	1.791	5403	5460	3571	307.1	1.810	5462	119.3	3549	1.810	
4	B2-17	1.605	11.48	116.5	118.5	3479	303.1	1.817	1.786	5367	5459	3558	306.1	1.817	5425	117.7	3515	1.817	
5	B2-19	1.597	11.41	115.9	117.8	3461	303.3	1.816	1.787	5372	5460	3583	306.2	1.816	5429	117.1	3496	1.816	
6	B2-20	1.596	11.42	116.0	117.8	3461	303.2	1.815	1.787	5372	5459	3581	306.3	1.815	5434	117.3	3500	1.815	
	avg	1.605	11.46	116.7	118.2	3472	303.2	1.810	1.788	5387	5456	3572	306.2	1.810	5443	117.9	3509	1.810	
								Phase III											
1	C1-01	1.618	11.51	119.1	---	3526	306.3	1.797	---	5485	---	3553	306.3	1.797	5489				1.00
2	C2-01	1.604	11.58	119.2	---	3558	307.3	1.812	---	5456	---	3582	307.2	1.812	5460				
3	C3-01	1.596	11.59	119.7	---	3571	308.1	1.814	---	5464	---	3580	308.1	1.814	5468				
	avg	1.606	11.56	119.3	---	3552	307.2	1.808	---	5468	---	3572	307.2	1.808	5472				
								Phase IV											
1	D4-15	---	---	117.9	---	3430	---	1.767	---	---	---					117.9	3430	1.767	1.00
2	D4-16	---	---	117.5	---	3427	---	1.772	---	---	---					117.5	3427	1.772	
3	D4-17	---	---	117.8	---	3587	---	1.849	---	---	---					117.8	3587	1.849	
4	D4-18	---	---	118.6	---	3562	---	1.824	---	---	---					118.6	3562	1.824	
	avg	---	---	117.9	---	3501	---	1.803	---	---	---					117.9	3501	1.803	

TABLE V
PERFORMANCE DATA ADJUSTMENT AT 20 SEC

Item	Firing No.	M. R.	$\dot{W}_T$, $\frac{lb_m}{sec}$	P_{cc_i}, psia	F_∞, lb_f	I_{sp_∞}, $\frac{lb_f\text{-sec}}{lb_m}$	C_{F_i}	c^*_i, $\frac{ft}{sec}$	$F_{\infty adj}$, lb_f	$I_{sp_{adj}}$, $\frac{lb_f}{lb_m/sec}$	$C_{F_{adj}}$	c^*_{adj}, $\frac{ft}{sec}$	$\frac{A^*_{calc}}{A^*_{initial}}$
PHASE I													
1	01-03	1.624	10.91	100.0	3370	308.4	1.771	—	—	309.2	—	—	0.992
2	02-02	1.629	11.21	102.4	3440	306.8	1.760	—	—	307.7	—	—	0.993
3	03-02	1.623	11.31	102.4	3475	307.2	1.778	—	—	308.0	—	—	0.995
4	04-02	1.625	10.92	98.9	3335	305.4	1.772	—	—	308.7	—	—	0.995
	avg	1.625	11.09	100.9	3405	307.0	1.770	—	—	308.4	—	—	0.994
PHASE II													
1	B1-5	1.634	11.48	117.3	3475	302.8	1.802	5404	3555	305.9	1.802	5467	1.000
2	B1-8	1.621	11.38	116.2	3442	302.6	1.802	5400	3555	305.4	1.802	5457	
3	B2-13	1.578	11.56	118.1	3514	304.0	1.810	5403	3571	307.1	1.810	5462	
4	B2-17	1.605	11.48	116.5	3479	303.1	1.817	5367	3558	306.1	1.817	5425	
5	B2-19	1.597	11.41	115.9	3461	303.3	1.816	5372	3583	306.2	1.816	5429	
6	B2-20	1.596	11.42	116.0	3461	303.2	1.815	5372	3581	306.3	1.815	5434	
	avg	1.605	11.46	116.7	3472	303.2	1.810	5387	3572	306.2	1.810	5443	
PHASE III													
1	C1-01	1.586	11.30	119.1	3481	308.1	1.807	5485	3509	308.1	1.807	5489	0.982
2	C1-02	1.596	11.12	120.8	3434	308.7	1.806		3414	309.2	1.806		0.956
3	C2-01	1.579	11.40	118.8	3537	310.2	1.824	5456	3574	310.2	1.824	5476	0.991
4	C2-02	1.601	11.27	119.0	3473	308.1	1.817		3502	308.0	1.817		0.975
5	C3-01	1.575	11.38	119.5	3526	309.8	1.821	5464	3539	309.6	1.821	5476	0.985
6	C3-02	1.538	11.19	121.2	3454	308.5	1.818		3423	309.2	1.818		0.954
	avg	1.579	11.28	119.7	3484	308.9	1.815	5468	3494	309.1	1.815	5480	0.974

UNCLASSIFIED

Security Classification

DOCUMENT CONTROL DATA - R&D

(Security classification of title, body of abstract and indexing annotation must be entered when the overall report is classified)

1. ORIGINATING ACTIVITY *(Corporate author)*
Arnold Engineering Development Center
ARO, Inc., Operating Contractor
Arnold AF Station, Tennessee

2a. REPORT SECURITY CLASSIFICATION
[redacted]

2b. GROUP
4

3. REPORT TITLE
SUMMARY OF THE ALTITUDE DEVELOPMENT TESTING OF THE BELL MODEL 8258 ROCKET ENGINE IN THE PROPULSION ENGINE TEST CELL (J-2A) (LEM ASCENT STAGE PRIMARY PROPULSION SYSTEM)

4. DESCRIPTIVE NOTES *(Type of report and inclusive dates)*
Summary Report

5. AUTHOR(S) *(Last name, first name, initial)*
Matkins, E. H. and Farrow, K. L., ARO, Inc.

6. REPORT DATE	7a. TOTAL NO. OF PAGES	7b. NO. OF REFS
June 1965	68	9

8a. CONTRACT OR GRANT NO.
AF 40(600)-1000

b. PROJECT NO.
9071

c. Program Area 921E

d.

9a. ORIGINATOR'S REPORT NUMBER(S)
AEDC-TR-65-97

9b. OTHER REPORT NO(S) *(Any other numbers that may be assigned this report)*
N/A

10. AVAILABILITY/LIMITATION NOTICES
Qualified requesters may obtain copies of this report from DDC.

11. SUPPLEMENTARY NOTES
N/A

12. SPONSORING MILITARY ACTIVITY
Manned Spacecraft Center, National Aeronautics and Space Administration, Houston, Texas

13. ABSTRACT

The development test program of the LEM Ascent Stage Primary Propulsion System was conducted in the Propulsion Engine Test Cell (J-2A). This program was designed to determine the performance, thermal characteristics, and durability of two configurations of the engine at a pressure altitude of approximately 100,000 ft. One configuration of the engine was operated at a chamber pressure of 100 psia and the other at 120 psia. Included in the program were (1) a simulated mission duty cycle for both configurations of the all-ablative engines, (2) a survey of engine performance as a function of chamber pressure, chamber length, and mixture ratio utilizing an all-metal engine of the 120-psia chamber pressure configuration, and (3) a study of the proposed LEM Ascent Staging technique using an all-ablative 120-psia chamber pressure engine. (U)

DD FORM 1 JAN 64 1473

UNCLASSIFIED

Security Classification

14. KEY WORDS	LINK A		LINK B		LINK C	
	ROLE	WT	ROLE	WT	ROLE	WT
Lunar Excursion Module (LEM) Ascent Stage Rocket Altitude Testing Rocket Motors Performance Thermal Characteristics Durability						

INSTRUCTIONS

1. ORIGINATING ACTIVITY: Enter the name and address of the contractor, subcontractor, grantee, Department of Defense activity or other organization *(corporate author)* issuing the report.

2*a*. REPORT SECURITY CLASSIFICATION: Enter the overall security classification of the report. Indicate whether "Restricted Data" is included. Marking is to be in accordance with appropriate security regulations.

2*b*. GROUP: Automatic downgrading is specified in DoD Directive 5200.10 and Armed Forces Industrial Manual. Enter the group number. Also, when applicable, show that optional markings have been used for Group 3 and Group 4 as authorized.

3. REPORT TITLE: Enter the complete report title in all capital letters. Titles in all cases should be unclassified. If a meaningful title cannot be selected without classification, show title classification in all capitals in parenthesis immediately following the title.

4. DESCRIPTIVE NOTES: If appropriate, enter the type of report, e.g., interim, progress, summary, annual, or final. Give the inclusive dates when a specific reporting period is covered.

5. AUTHOR(S): Enter the name(s) of author(s) as shown on or in the report. Enter last name, first name, middle initial. If military, show rank and branch of service. The name of the principal author is an absolute minimum requirement.

6. REPORT DATE: Enter the date of the report as day, month, year; or month, year. If more than one date appears on the report, use date of publication.

7*a*. TOTAL NUMBER OF PAGES: The total page count should follow normal pagination procedures, i.e., enter the number of pages containing information.

7*b*. NUMBER OF REFERENCES: Enter the total number of references cited in the report.

8*a*. CONTRACT OR GRANT NUMBER: If appropriate, enter the applicable number of the contract or grant under which the report was written.

8*b*, 8*c*, & 8*d*. PROJECT NUMBER: Enter the appropriate military department identification, such as project number, subproject number, system numbers, task number, etc.

9*a*. ORIGINATOR'S REPORT NUMBER(S): Enter the official report number by which the document will be identified and controlled by the originating activity. This number must be unique to this report.

9*b*. OTHER REPORT NUMBER(S): If the report has been assigned any other report numbers *(either by the originator or by the sponsor)*, also enter this number(s).

10. AVAILABILITY/LIMITATION NOTICES: Enter any limitations on further dissemination of the report, other than those imposed by security classification, using **standard statements** such as:

(1) "Qualified requesters may obtain copies of this report from DDC."

(2) "Foreign announcement and dissemination of this report by DDC is not authorized."

(3) "U. S. Government agencies may obtain copies of this report directly from DDC. Other qualified DDC users shall request through _____."

(4) "U. S. military agencies may obtain copies of this report directly from DDC. Other qualified users shall request through _____."

(5) "All distribution of this report is controlled. Qualified DDC users shall request through _____."

If the report has been furnished to the Office of Technical Services, Department of Commerce, for sale to the public, indicate this fact and enter the price, if known.

11. SUPPLEMENTARY NOTES: Use for additional explanatory notes.

12. SPONSORING MILITARY ACTIVITY: Enter the name of the departmental project office or laboratory sponsoring *(paying for)* the research and development. Include address.

13. ABSTRACT: Enter an abstract giving a brief and factual summary of the document indicative of the report, even though it may also appear elsewhere in the body of the technical report. If additional space is required, a continuation sheet shall be attached.

It is highly desirable that the abstract of classified reports be unclassified. Each paragraph of the abstract shall end with an indication of the military security classification of the information in the paragraph, represented as *(TS)*, *(S)*, *(C)*, or *(U)*.

There is no limitation on the length of the abstract. However, the suggested length is from 150 to 225 words.

14. KEY WORDS: Key words are technically meaningful terms or short phrases that characterize a report and may be used as index entries for cataloging the report. Key words must be selected so that no security classification is required. Identifiers, such as equipment model designation, trade name, military project code name, geographic location, may be used as key words but will be followed by an indication of technical context. The assignment of links, rules, and weights is optional.